Discovery of 7-Hydroxy-6-methoxy-2-methyl-3-(3,4,5-trimethoxybenzoyl)benzo[*b*]furan (BNC105), a Tubulin Polymerization Inhibitor with Potent Antiproliferative and Tumor Vascular Disrupting Properties

Bernard L. Flynn,*,[†,‡] Gurmit S. Gill,[†] Damian W. Grobelny,[†] Jason H. Chaplin,[†] Dharam Paul,[†] Annabell F. Leske,[†] Tina C. Lavranos,[†] David K. Chalmers,[‡] Susan A. Charman,[§] Edmund Kostewicz,[§] David M. Shackleford,[§] Julia Morizzi,[§] Ernest Hamel,[∥] M. Katherine Jung,[⊥] and Gabriel Kremmidiotis[†]

[†]Bionomics Ltd., 31 Dalgleish Street, Thebarton, South Australia, 5031, Australia

[‡]Medicinal Chemistry and Drug Action and [§]Centre for Drug Candidate Optimisation, Monash Institute of Pharmaceutical Sciences, Monash University, 381 Royal Parade, Parkville, 3052, Victoria, Australia

[∥]Screening Technologies Branch, Developmental Therapeutics Program, Division of Cancer Treatment and Diagnosis, National Cancer Institute at Frederick, National Institutes of Health, Frederick, Maryland 21702, United States

[⊥]Division of Metabolism and Health Effects, National Institute of Alcohol Abuse and Alcoholism, National Institutes of Health, Bethesda, Maryland 20892, United States

S Supporting Information

ABSTRACT: A structure−activity relationship (SAR) guided design of novel tubulin polymerization inhibitors has resulted in a series of benzo[*b*]furans with exceptional potency toward cancer cells and activated endothelial cells. The potency of early lead compounds has been substantially improved through the synergistic effect of introducing a conformational bias and additional hydrogen bond donor to the pharmacophore. Screening of a focused library of potent tubulin polymerization inhibitors for selectivity against cancer cells and activated endothelial cells over quiescent endothelial cells has afforded 7-hydroxy-6-methoxy-2-methyl-3-(3,4,5-trimethoxybenzoyl)benzo-[*b*]furan (BNC105, **8**) as a potent and selective antiproliferative. Because of poor solubility, **8** is administered as its disodium phosphate ester prodrug **9** (BNC105P), which is rapidly cleaved in vivo to return the active **8**. **9** exhibits both superior vascular disrupting and tumor growth inhibitory properties compared with the benchmark agent combretastatin A-4 disodium phosphate **5** (CA4P).

combretastatin A-4

potency x 10
selectivity x 80
half-life x 5
free drug fraction x 10
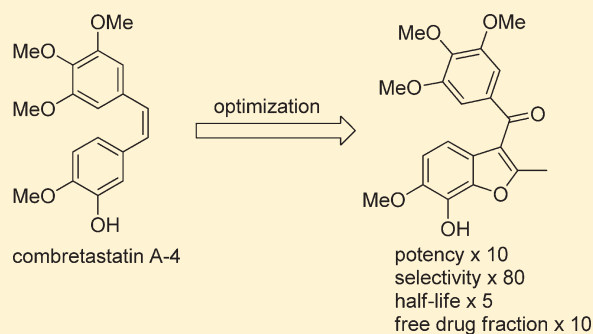
INTRODUCTION

Microtubules are protein biopolymers formed through polymerization of heterodimers of α- and β-tubulin.[1] The polymerization is reversible, and the dynamic assembly and disassembly of microtubules are involved in a number of cell functions, including cell division, migration, and shape change. Microtubules are also involved in a host of cell signaling pathways, including those related to apoptosis. Compounds that bind to α,β-tubulin heterodimers and disrupt the dynamics of microtubule assembly and disassembly have emerged as some of the most effective chemotherapeutics for the treatment of cancer. Notable examples include the *Catharanthus* (or vinca) alkaloids vinblastine and vincristine and the taxoids paclitaxel and docetaxel.[2] These drugs are powerful antimitotic agents that inhibit cancer cell proliferation and induce apoptosis. While they have proven to be successful in the treatment of cancer, their narrow therapeutic index and the emergence of resistance have inspired efforts to

search for safer and more effective agents that are capable of treating resistant phenotypes.[2]

The *Catharanthus* alkaloids and the taxoids bind at separate sites on the α,β-tubulin heterodimer, and another natural product, colchicine **1** (Figure 1), binds to a third distinct site.[1] Compounds that bind to the colchicine site have been the subject of intense investigation by researchers seeking to identify new agents capable of addressing the limitations of existing tubulin targeting drugs.[3,4] In addition to being potent antimitotics, compounds that bind to the colchicine site also show potent vascular disrupting properties, which result from the effects of these compounds on vascular endothelial cells.[5,6] Such vascular disrupting agents (VDAs) take advantage of the significant differences that exist between the vasculature of normal, healthy tissues and that of tumors. The selective shutdown of tumor
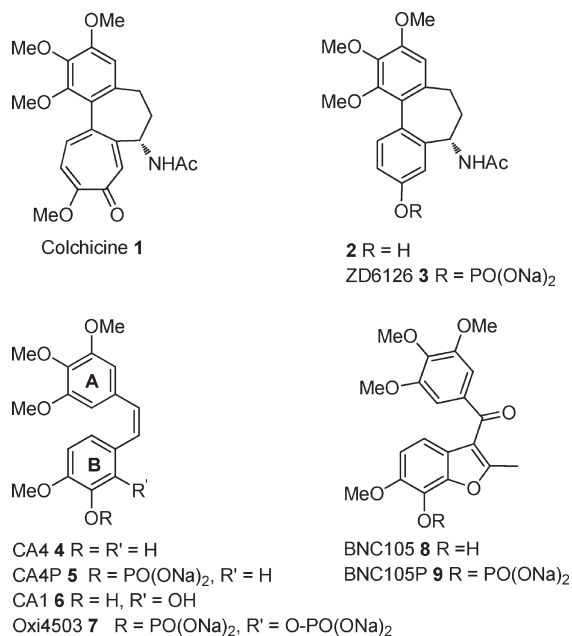
Figure 1. Tubulin binding agents with affinity for the colchicine site.

Colchicine **1**

2 R = H
ZD6126 **3** R = PO(ONa)₂

CA4 **4** R = R' = H
CA4P **5** R = PO(ONa)₂, R' = H
CA1 **6** R = H, R' = OH
Oxi4503 **7** R = PO(ONa)₂, R' = O-PO(ONa)₂

BNC105 **8** R =H
BNC105P **9** R = PO(ONa)₂

Table 1. SAR Studies of Tubulin Polymerization Inhibitors I

I, **10-13**   **14**   **15** (BPROL075)

| entry	compd	X	R	tubulin[a,b] IC₅₀ (μM)	MCF-7[b] IC₅₀ (nM)
1	**4**			1.8 ± 0.2	11 ± 4
2	**10**	S	H	>40[c]	2000
3	**11**	S	OH	3.4 ± 0.2	520 ± 400
4	**14**			1.0 ± 0.1	300 ± 400
5	**12**	O	OH	1.3 ± 0.2	39 ± 18
6	**13**	NH	OH	1.6 (both runs)	45 ± 5

[a] Inhibition of extent of microtubule assembly was the parameter measured. [b] All data were obtained from the same laboratory: refs 17–20. [c] The rate but not the extent of tubulin polymerization was inhibited by 50%.

vasculature starves tumors of oxygen and nutrients, leading to significant cancer cell death through necrosis and apoptotis. While the antimitotic and vascular disrupting properties of colchicine have been known for over 50 years, toxicity issues have prevented its clinical development as an anticancer agent. The significant toxicity of colchicine (LD₅₀ < 5 mg/kg in rodents) is attributed to its very slow dissociation from tubulin ($t_{1/2}$ = 35 h), which leads to persistence in sensitive tissues for several days.[7−9] Compounds that bind more reversibly to the colchicine site often have shorter half-lives in vivo and are much better tolerated.[10] N-Acetylcolchicinol **2** and combretastatin A-4 (CA4) **4** are examples of reversible binders to the colchicine site that have short half-lives in vivo and that are much better tolerated than colchicine.[5,6,10] Since vascular disruption in tumors peaks after just a few minutes, safe and effective vascular shutdown can be achieved by tubulin binders that have reversible binding kinetics and short half-lives. Both **2** and **4** have entered clinical trials, where they are administered as the soluble disodium phosphate ester prodrugs **3** (ZD6126) and **5** (CA4P), which are rapidly cleaved in vivo to the active agents.[10−12] A significant drawback of the short half-lives of **2** and **4** is that a short period of in vivo exposure is often insufficient to elicit a significant cell kill via the antimitotic effect of these compounds.[13] As a result, significant tumor growth from the outer rim of the tumor is maintained, since this region is often fed by normal, healthy vasculature and is not susceptible to the vasculature disrupting effects of tubulin binders.[14] The more potent tumor growth inhibitory properties of **7** (Oxi4503), a phosphate prodrug of combretastatin A-1 (CA1) **6**, are attributed to its capacity to act as both a VDA and a cytotoxic agent.[15] After in vivo deesterification of **7**, to give the short half-life VDA **6**, further metabolism occurs to produce a cytotoxic o-quinone (not shown).[15] Thus **7**, represents a dual mode agent capable of targeting the vasculature of the internal regions of the tumor and proliferative cancer cells of the viable rim.[15] Since tubulin binding compounds are cytotoxic in their own right, we considered that a moderate half-life agent might act as both a VDA and a cytotoxin

in vivo without exhibiting undue toxicity. In order to further offset any increase in toxicity that may result from a moderate increase in half-life, we also sought a selective compound that would exhibit higher potency toward cancer cells and tumor vascular endothelial cells relative to normal, healthy tissues. These efforts have led to the identification of **8** (BNC105), and we have recently described aspects of this compound's vascular disrupting and tumor growth inhibitory properties in animal models.[16] Herein, we describe the SAR-guided discovery process that led to **8** and the key biological data that led to its selection as a candidate for further development, including its potency and selectivity toward various cancer cell lines, effectiveness against multidrug resistant phenotypes, and favorable pharmacokinetics.[17]

■ RESULTS AND DISCUSSION

Background SAR. Early studies by Pinney and co-workers identified benzo[b]thiophene **10** as weak inhibitor of tubulin polymerization that binds to the colchicine binding site (entry 2, Table 1).[18] X-ray crystal structure analysis of **10** revealed the A-ring to be rotated toward the D-ring in a pseudo-π-stacking arrangement.[18b] It was concluded that this conformation is likely to be important to binding, and early SAR studies within our group indicated that the A- and D-rings of **10** may coincide with the A- and B-rings of **4**.[18−20] For example, the introduction of a 3′-hydroxyl to the D-ring of **10** (compound **11**) increased structural analogy to **4** and increased potency (entry 3, Table 1). Also, removal of the B-ring in **11** was well tolerated, giving an even more potent compound **14** (entry 4, Table 3). On the other hand, we also found that small changes in the substitution pattern of the B-ring of **10**, such as removal or relocation of the C6-methoxy to C5, completely eliminated activity, indicating that the B-ring does contribute to activity when present (data not shown).[19] We also identified that the benzo[b]furan **12** and indole **13** analogues of benzo[b]thiophene **11** were much more potent (compare entries 3, 5, and 6, Table 1) and that for all systems **I** (X = O, S, NH) the carbonyl linker between the A- and C-rings is essential for activity (data not shown).[21,22] Later, Hseih
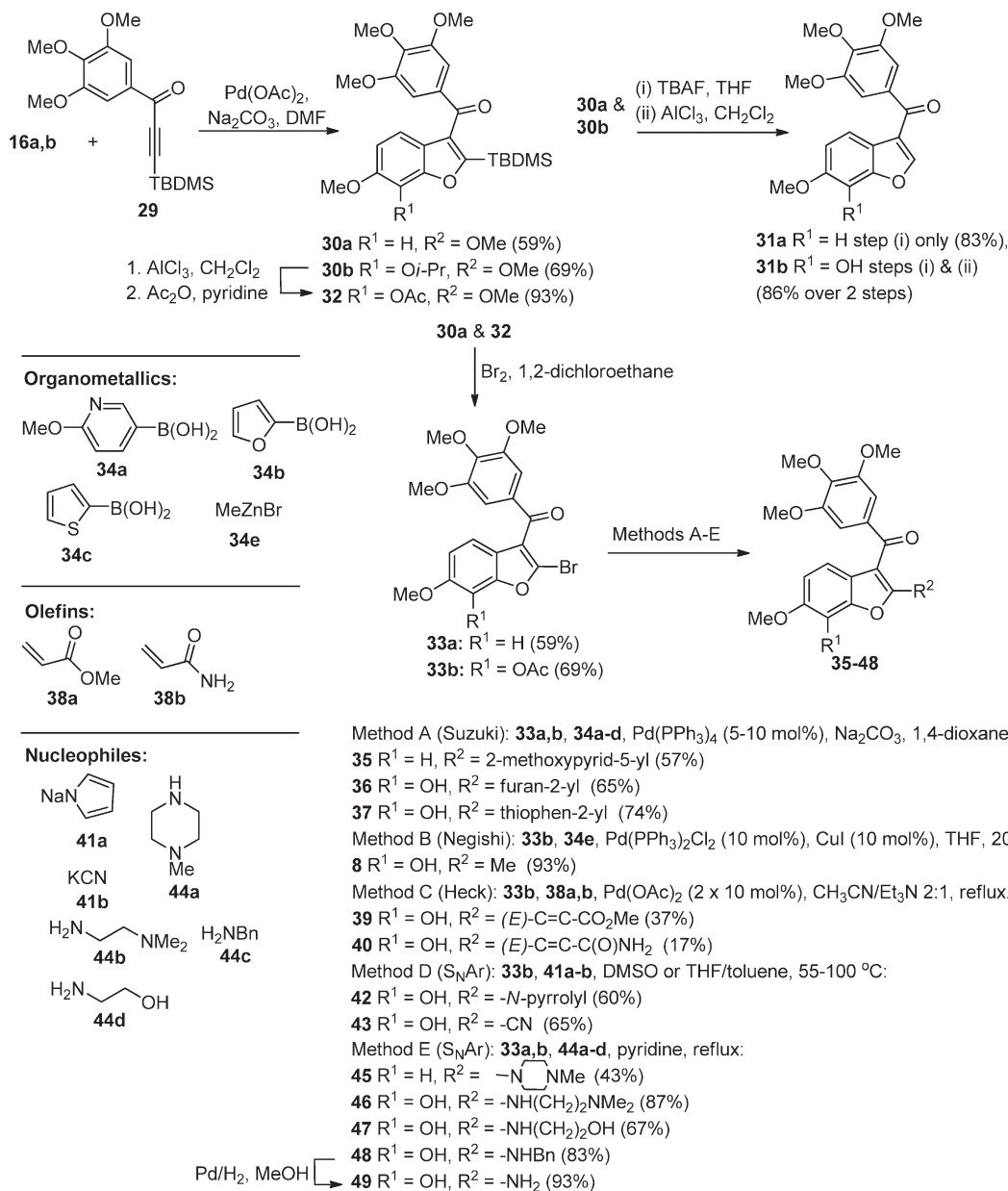
Table 2. MCC Reaction
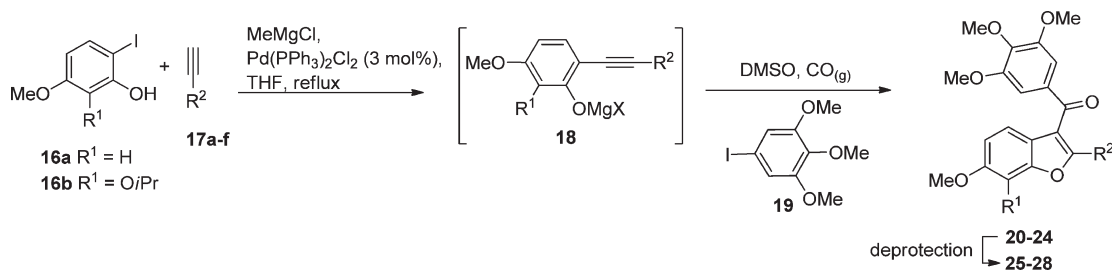
entry	16 R^1	17 R^2	product (yield%)	deprotection conditions	product (yield%) R^1, R^2
1	**16a** H	**17a**	**20** (31)	Pd/C, H$_2$ (g)	**25** (34) R^1 = H,
2	**16a** H	**17b**	**21** (32)	–	–
3	**16a** H	**17c**	**22** (30)	Pd/C, H$_2$ (g)	**26** (63) R^1 = H,
4	**16b** OiPr	**17d**	**23** (46)	AlCl$_3$, CH$_2$Cl$_2$	**27** (51) R^1 = OH,
5	**16b** OiPr	**17f**	**24** (55)	AlCl$_3$, CH$_2$Cl$_2$	**28** (75) R^1 = OH,

and co-workers reported that indole **15** (BPROL075), an analogue of **13** in which the D-ring is absent, is also active.[23] On the basis of similarities in the SAR of **15** and **4**, they concluded that the A- and B-rings of **15** correlate with the A- and B-rings of **4**. These results presented the possibility that the D-ring in compounds **I** (**10**−**13**) may be redundant and that in fact the B-ring in **I** plays an equivalent role to the B-ring of **4**. On the other hand, π-stacking interactions between the A- and D-rings in **I** may induce a conformational change such that compounds **I** present a different pose to the tubulin binding site than does **15**, that is, where the A- and D-rings in **I** equate to the A- and B-rings of **4**. Therefore, in order to understand the SAR and generate more potent analogues of **I** and **15**, a closer evaluation of the relative contributions of the B- and D-rings in **I** would be required. Since benzo[*b*]furans generally gave the

most effective leads, based on potency and stability (metabolic and thermal), we focused our investigations on **I** (X = O).

Compound Synthesis. The compounds generated in the course of this work were prepared either by use of a multi-component coupling (MCC) reaction or by a modified Larock-type coupling (Table 2 and Scheme 1).[17,24,25] The one-pot MCC reaction involves deprotonation of an *o*-iodophenol **16** and a terminal alkyne **17** with methylmagesium chloride to generate a magnesium phenolate and magnesium acetylide that then couple to give **18** in the presence of a catalytic amount of Pd(PPh$_3$)$_2$Cl$_2$ (3 mol %) in THF at reflux (Table 2). The THF is then exchanged for DMSO. The third coupling partner, aryl iodide **19**, is introduced and the reaction mixture heated under an atmosphere of CO (g) (balloon). This produces a carbonylative, heteroannulative coupling reaction between **18** and **19**, giving the

Scheme 1. Modified Larock Coupling

Organometallics:

34a · 34b · 34c · MeZnBr 34e

Olefins:

38a · 38b

Nucleophiles:

NaN 41a · KCN 41b · 44a · H₂N NMe₂ 44b · H₂NBn 44c · H₂N OH 44d

Pd/H₂, MeOH

Method A (Suzuki): **33a,b**, **34a-d**, Pd(PPh₃)₄ (5-10 mol%), Na₂CO₃, 1,4-dioxane / H₂O, reflux:
35 R¹ = H, R² = 2-methoxypyrid-5-yl (57%)
36 R¹ = OH, R² = furan-2-yl (65%)
37 R¹ = OH, R² = thiophen-2-yl (74%)
Method B (Negishi): **33b**, **34e**, Pd(PPh₃)₂Cl₂ (10 mol%), CuI (10 mol%), THF, 20 °C:
8 R¹ = OH, R² = Me (93%)
Method C (Heck): **33b**, **38a,b**, Pd(OAc)₂ (2 x 10 mol%), CH₃CN/Et₃N 2:1, reflux.
39 R¹ = OH, R² = (E)-C=C-CO₂Me (37%)
40 R¹ = OH, R² = (E)-C=C-C(O)NH₂ (17%)
Method D (S_NAr): **33b**, **41a-b**, DMSO or THF/toluene, 55-100 °C:
42 R¹ = OH, R² = -N-pyrrolyl (60%)
43 R¹ = OH, R² = -CN (65%)
Method E (S_NAr): **33a,b**, **44a-d**, pyridine, reflux:
45 R¹ = H, R² = −N‿NMe (43%)
46 R¹ = OH, R² = -NH(CH₂)₂NMe₂ (87%)
47 R¹ = OH, R² = -NH(CH₂)₂OH (67%)
48 R¹ = OH, R² = -NHBn (83%)
49 R¹ = OH, R² = -NH₂ (93%)

3-aroylbenzo[b]furans **20−24** in moderate yields (30−55%).[17] This step involves initial oxidative insertion of the palladium into the C−I bond of **19**, followed by CO insertion to give an electrophilic ArC(O)PdI complex that coordinates to the alkyne bond of **18**, promoting cyclization to give a 3-[ArC(O)Pd]-benzo[b]furan complex. Reductive elimination then affords the 3-aroylbenzo[b]furans **20−24**. A number of products **20−24** required deprotection in order to afford the desired test compounds. The benzyl protecting groups in **20** and **22** were cleaved by hydrogenation to give **25** (34%) and **26** (63%), respectively.[17] The isopropyl ether protecting groups in **23** and **24** were cleaved using AlCl₃ in dichloromethane, giving **27** (51%) and **28** (75%), respectively.[17]
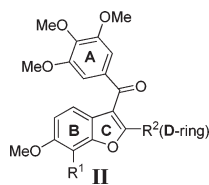
In order to better explore the SAR of the C2 position of the benzo[b]furan lead series (see below) and to aid in the generation of a focused library of active compounds, we devised a concise method for the preparation of 2-substituted benzo[b]-furans (Scheme 1). This approach involves a modified Larock-type coupling between o-iodophenol **16a,b** and the 3-silyl-1-arylpropynone **29** to give 2-silylbenzo[b]furans **30a,b**.[25,26] Silanes **30a,b** were subjected to treatment with TBAF in methanol to remove the silyl groups and, in the case of **30b**, reaction with AlCl₃, to remove the isopropyl group, giving **31a** and **31b** in good yields (83% and 86%, respectively). Bromo-desilylation of **30a** was achieved in reasonable yield to give the 2-bromobenzo-[b]furan **33a** (59%).[25] In the case of **30b**, it was necessary to first exchange an isopropyl for an acetyl group (**32**) in order to avoid competitive C4-bromination of the benzo[b]furan in the bromo-desilylation step. Subsequent conversion of **32** to bromide **33b** proceeded smoothly (69%).[25] The bromo substituent in **33a** and **33b** proved to be a versatile functionality that could be readily substituted by way of palladium mediated coupling or by nucleophilic displacement to produce a host of analogues **35−48**

(Methods A−E).[17,25] The acetyl group was generally cleaved under the reaction conditions used for C2-substitution or by methanolysis (MeOH, K_2CO_3) of the crude product. In the case of **48**, hydrogenation of the benzyl substituent was required to afford the desired test compound, amine **49**.[17]
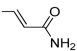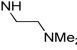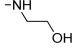
Biological Evaluation. The endothelial cells within tumors are constantly exposed to proangiogenic growth factors and, as a consequence, are in a constant state of activation and angiogenesis.[27] Since we were primarily interested in identifying a new compound capable of selective inhibition of tumor over normal

Table 3. Biological Evaluation of Benzo[b]furans II

entry	cmpnd	R^1	R^2(D-ring)	tubulin[a] IC_{50} (µM)	MCF-7[b] IC_{50} (nM)	activated HUVEC[c] IC_{50} (nM)	quiescent HUVEC[d] IC_{50} (nM)	selectivity ratio[e]
1	**4**	-	-	1.8 ± 0.2	2.9	3.6	3.9	1.1
2	**12**	H	(phenyl, OH, OMe)	1.3± 0.2	39±18	45	41	0.9
3	**21**	H	(indole, NMe)	1.3 ± 0.04	42±10	41	32	0.8
4	**25**	H	(phenyl, NH2, OMe)	1.9 ± 0.4	26±5	32	44	1.4
5	**26**	H	(phenyl, OH)	2.3 (both runs)	48±10	30	34	1.1
6	**31a**	H	H	1.6 ± 0.2	55±5	45	63	1.4
7	**31b**	OH	H	ND	45 ±15	83	322	3.9
8	**27**	OH	(phenyl, OH, OMe)	0.8± 0.2	4.0±0.1	1.7	3.4	2.0
9	**8**	OH	Me	3.0± 0.6	2.4±2	0.31	25	81
10	**28**	OH	(pyrazole, NMe)	1.3 ± 0.07	1.0±0.5	0.4	0.7	1.8
11	**24**	O*i*Pr	(pyrazole, NMe)	ND	42±6	665	419	0.6
12	**33a**	H	Br	ND	495±25	510	309	0.6
13	**35**	H	(pyridine, OMe)	ND	71±1	45	27	0.6
14	**45**	H	(N-piperazine, NMe)	ND	215±15	484	405	0.8
15	**36**	OH	(furan)	8.7 ± 0.8	0.6±0.2	3.6	3.4	0.9
16	**37**	OH	(thiophene)	ND	0.5±0.2	0.31	0.36	1.2
17	**42**	OH	(N-pyrrole)	ND	ND	2.6	3.3	1.3
18	**39**	OH	(vinyl, CO2Me)	ND	ND	0.38	2.3	6.0
19	**43**	OH	CN	ND	ND	1.1	3.0	2.7

Table 3. Continued

entry	cmpnd	R^1	R^2(D-ring)	tubulin[a] IC_{50} (μM)	MCF-7[b] IC_{50} (nM)	activated HUVEC[c] IC_{50} (nM)	quiescent HUVEC[d] IC_{50} (nM)	selectivity ratio[e]
20	**40**	OH	(structure)	ND	ND	2.6	2.3	0.9
21	**46**	OH	(structure)	ND	ND	29	36	1.2
22	**47**	OH	(structure)	ND	ND	3.1	2.9	0.9
23	**49**	OH	NH_2	ND	ND	1.9	8.8	4.6

[a] The tubulin concentration was 10 μM. Inhibition of extent of assembly was the parameter measured ($n = 2$). [b] Cells were grown for 48 h at 37 °C in a humidified 5% CO_2 atmosphere. Cell protein was the parameter measured. At least two independent experiments were performed with each compound. [c] For activated growth conditions HUVEC cells were seeded at 2500 and 500 cells/well, respectively, and cultured in EGM-2 medium (Lonza) or F12K medium containing 0.03 mg/mL endothelial cell growth supplement. [d] For quiescent growth conditions HUVEC and HAAE-1 cells were seeded at 15 000 and 5000 cells/well, respectively, in basal medium (EBM-2 or F12K) containing 0.5% fetal calf serum and antibiotics. [e] Selectivity ratio (IC_{50} quiescent)/(IC_{50} activated).

endothelial cells, all new compounds were screened for their capacity to selectively inhibit human umbilical vein endothelial cells (HUVECs) grown in the presence (activated) or absence (quiescent) of growth factors (Table 3). Key compounds were also evaluated for their capacity to inhibit tubulin polymerization and the proliferation of MCF-7 cancer cells (Table 3).

In our SAR studies of the benzo[*b*]furan lead structure **II** (Table 3), we first sought to investigate whether the presence of a C2-aryl group (D-ring) in **II** influences its mode of binding and which of the two rings B or D in **II** equates to the B-ring in **4**. To do this, we generated three new D-ring analogues of **12**, compounds **21**, **25**, and **26**, all of which should be capable of a similar pseudo-π-stacking interaction with the A-ring as seen in the crystal structure of **10** (entries 3–5, Table 3). If the D-ring in **II** plays the role of the B-ring in **4**, then based on previous SAR studies of **4**,[28–30] compounds **25** and **21** should be of similar potency to **12**, whereas **26** should be inactive. However, all new analogues **21**, **25**, **26** exhibited similar potency to **12** (compare entries 2–5, Table 3). Furthermore, these compounds were all of similar potency to the C2-unsubstituted analogue **31a** (a benzo-[*b*]furan equivalent of **15**) (compare entries 2–6, Table 2). These data indicate that while the D-ring in **II** is tolerated, it does not contribute to the potency of this series. Most likely, all compounds **II** present a similar pose to tubulin irrespective of whether a C2-aryl substituent (D-ring) is present or not (see also docking studies below). Thus, the B-ring in **I/II** plays an equivalent role to the B-ring in **4** and the presence of a C2-aryl does not influence this conformation. This is also consistent with our earlier observation that a C6-methoxy is required for the potency of **I** (X = S), even when a C2-aryl is present.[19] An alternative explanation for the increase in potency of **11** relative to **10** (entries 2 and 3, Table 2) may be that the inhibitory effects of **10** are limited by poor solubility at higher assay concentrations and that the presence of a hydroxyl in **11** improves solubility.

Satisfied that the B-ring in **II** corresponds to the B-ring in **4**, irrespective of the presence of a C2-aryl, we next investigated the effect of introducing a hydroxyl group ortho to the C6-methoxy in **31a** and **12**, giving **31b** and **27**, respectively (entries 7 and 8, Table 3). We introduced the hydroxyl to the C7-position rather than the C5-position, since superimposing **4**, colchicine, and **31b**

indicated that this would be the most appropriate location (Figure 2). The introduction of a C7-OH to **31a**, giving **31b**, was tolerated and afforded a compound of similar potency to **31a**, which was slightly more selective for activated over quiescent endothelial cells (entry 7, Table 3). This is consistent with the SAR of **4**, where removal of the B-ring hydroxyl has little effect on potency.[30] Interestingly, the introduction of a C7-OH to indole **15** has recently been shown to reduce potency (∼20-fold increase in IC_{50} values across multiple cell lines), albeit to a lesser degree than a C5-OH.[31] While **31a** and **31b** are of similar potency, the introduction of a C7-OH to **12** afforded a much more potent compound, **27** (compare entries 2 and 8, Table 3). This 10-fold increase in potency is not attributed to any particular pharmacophoric feature of the C2-aryl in **27**, as many other C2-substituted systems bearing a C7-OH exhibit similar levels of potency (compare entries 8–23, Table 3). Moreover, the SAR data accumulated in this study indicate a synergistic (>additive) effect for the introduction of *both* a C7-OH and a C2-substituent. This synergism is apparent for a range of different C2-substitutents where the antiproliferative activity of lead series **II** exhibits a SAR as follows: $[R^1 = OH, R^2 \neq H] \gg [R^1 = H, R^2 = H] \approx [R^1 = OH, R^2 = H] \approx [R^1 = H, R^2 \neq H]$ (compare entries 2, 6, 7, and 8, Table 3)

Presumably, the C2-substituent in **II** plays a steric role, favoring cisoid-**II** over transoid-**II** because of increased steric compression in the latter, forcing the A- and B-rings into the preferred orientation for binding to tubulin (Figure 3). This is supported by quantum chemical calculations on **31b** (**II**, R^1 = OH, R^2 = H) and **8** (**II**, R^1 = OH, R^2 = Me). Calculations using the B3LYP method with the 6-311g** basis set show that although the energy differences are not large, in **31b** the transoid conformation is favored by 1.1 kJ/mol while in compound **8** the cisoid conformation is favored by 0.3 kJ/mol.

Generally speaking, both hydrophobic and hydrophilic substituents are well tolerated in the C2-position of **II**, giving potent antiproliferative compounds in most cases, particularly for C7-OH analogues (entries 7–23, Table 3).[32] Nonetheless, some C2 substituents had significant effects on potency. The presence of a strong base at C2, as in compounds **45** and **46**, tended to reduce potency (entries 14 and 21, respectively, Table 3). At this stage, it is uncertain as to whether this is as a result of reduced affinity of
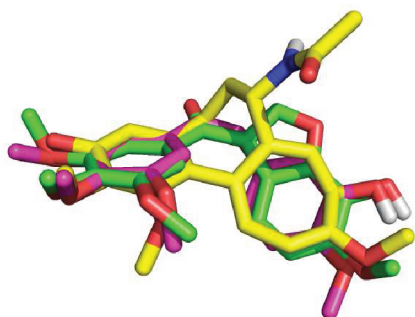
Figure 2. Superpositioning of colchicine **1** (yellow), **4** (pink), and **27a** (green). Oxygen atoms are red. Nitrogen atoms are blue.
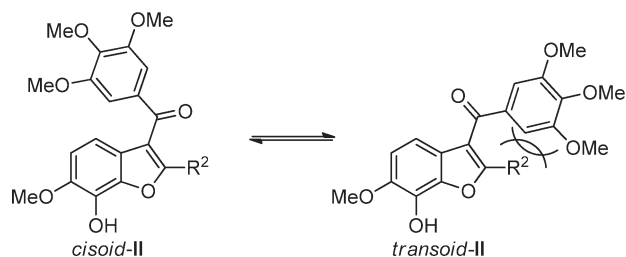

Figure 3. Cisoid and transoid rotamers of **II**.

these compounds for the target or due to partial sequestration of the active into acidic vesicles in the cell, reducing the concentration in the proximity of the microtubules. Additionally, certain five-membered ring heterocycles in the C2-position, furan **36**, thiophene **37**, and *N*-methylpyrazole **28**, afforded very potent compounds (entries 10, 15, and 16, respectively, Table 3). Of all the C2-substitutients evaluated,[32] only the C2-methyl **8** showed any significant selectivity for activated HUVECs over quiescent HUVECs (81-fold) (entry 9, Table 3). **8** also exhibited good potency against MCF-7 cancer cells (IC_{50} = 2.4 nM).

Notwithstanding that there is some variation in activity and selectivity as a function of C2-substitution in **II**, the broader tolerance to structural variation at this position indicates that it is probably oriented away from the binding pocket, directing its substituent into an area of relative "free space" (solvent water).[32] This and other features of the SAR were supported by docking studies. Using the X-ray crystal structure of bovine α,β-tubulin dimer complexed to podophylotoxin (PDB entry 1SA1),[33] we used Glide[34] to dock a variety of benzo[*b*]furan compounds into the colchicine site (Figure 4), which lies within the β-tubulin subunit adjacent to its interface with α-tubulin.[35] The docked structures were oriented so that their 3,4,5-trimethoxyphenyl (A) rings overlapped with that of colchicine and the C6-OMe and C7-OH substituents overlapped with the methoxy and carbonyl groups on the tropone ring of colchicine. The benzo[*b*]furan C7-OH group makes a hydrogen bond to the side chain of Asn β258, which also forms a hydrogen bond to the backbone amide nitrogen of Val 181 in the adjacent α-tubulin subunit. The C2-position of the benzo[*b*]furan is oriented toward a gap between the α- and β-tubulin subunits which can accommodate large substituents. The D-ring of compound **27** projects into this gap, lying between residues Thr α179 and Leu β248.

In light of the favorable potency and selectivity exhibited by **8**, we subjected this compound to further in vitro and in vivo

biological evaluation. Compound **8** exhibited excellent potency against a panel of different cancer cell lines (Table 4). The selectivity observed for **8** against activated over quiescent HUVECs was also observed in human aortic arterial endothelial cells (HAAECs). Again, this selectivity was not seen with **4**. Furthermore, **8** generally exhibited greater potency than **4**, up to 10-fold in most cases.

We also evaluated **8** for multidrug resistance. Acquired resistance of human cancer cells to chemotherapeutic agents is one of the major causes of treatment failure.[36] A key mechanism of acquired resistance is the increased expression of the transporter, multidrug resistance protein MDR-1 (P-glycoprotein). This transporter effluxes drug agents from the cytoplasm of the cell, reducing the drug concentration to ineffective levels. Since more than 80% of current chemotherapeutics are substrates for MDR-1, it is important to identify new chemotherapeutic agents that are not MDR-1 substrates and that are able to treat multidrug resistant phenotypes. The renal carcinoma cell line 786-0 has high levels of expression of MDR-1, and the potency of drugs that are MDR-1 substrates is significantly reduced by this transporter. The three key tubulin targeting drugs paclitaxel, vincristine, and vinblastine are all known to be MDR-1 substrates and show enhanced activity against 786-0 when coadministered with the MDR-1 inhibitor verapamil (Table 5). By contrast, **8** was equipotent against 786-0 cells with and without verapamil, indicating that **8** is not a substrate for the MDR-1 transporter (Table 5).

MDR-1 overexpression is also a key element of the multidrug resistance acquired by the human ovarian cancer cell line A2780 upon continuous exposure to adriamycin, producing the A2780ADR phenotype.[37] Both doxorubicin and cisplatin, which are MDR-1 substrates, showed reduced potency toward this cell line, whereas **8** exhibited similar potency against both A2780 and A2780ADR (Table 6). Compound **8** also exhibited good potency toward the cisplatin resistant cell line A2780cis (Table 6). A2780cis cells exhibit cross-resistance to a number of cytotoxins and radiation in an MDR-1 independent manner.[37]

In order to achieve a dual mode agent, capable of acting as a VDA and an antimitotic, we were interested in producing a compound that exhibits increased exposure relative to **4** to improve cell kill levels through the antimitotic effect. Compared with **4**, **8** exhibits a longer half-life and larger $AUC_{0-\infty}$ in pharmacokinetic studies in rats (Table 7). It also exhibits a lower level of plasma protein binding (PPB) than **4**, resulting in a significantly higher free drug exposure of **8** relative to **4**. This increased exposure is expected to produce an increased cell kill through the antimitotic effect of **8**, particularly at the viable rim of the tumor that survives vascular disruption.

The poor aqueous solubility of **8** necessitated its conversion to the disodium phosphate ester **9**, providing a soluble prodrug for in vivo administration (Scheme 2), as has been done for **4** (**5**) and **2** (**3**) (Figure 1).[38] Prodrug **9** was prepared from **8** by carbon tetrabromide mediated esterification with dibenzyl phosphite to give the dibenzyl phosphate ester **50**. Ester **50** was converted to **9** upon sequential treatment with trimethylsilyl bromide and sodium methoxide. Pharmacokinetic evaluation of **9** in rats and mice revealed that it is rapidly converted to **8** and that it achieves similar levels of drug exposure (tumor and other tissues) compared to direct administration of **8**.[39]

In our previous report on the in vivo efficacy of **9** in murine tumor models, we demonstrated that **9** was more effective at tumor vasculature disruption than the disodium phosphate prodrug of combretastatin A-4 **5**. Also, in head-to-head studies
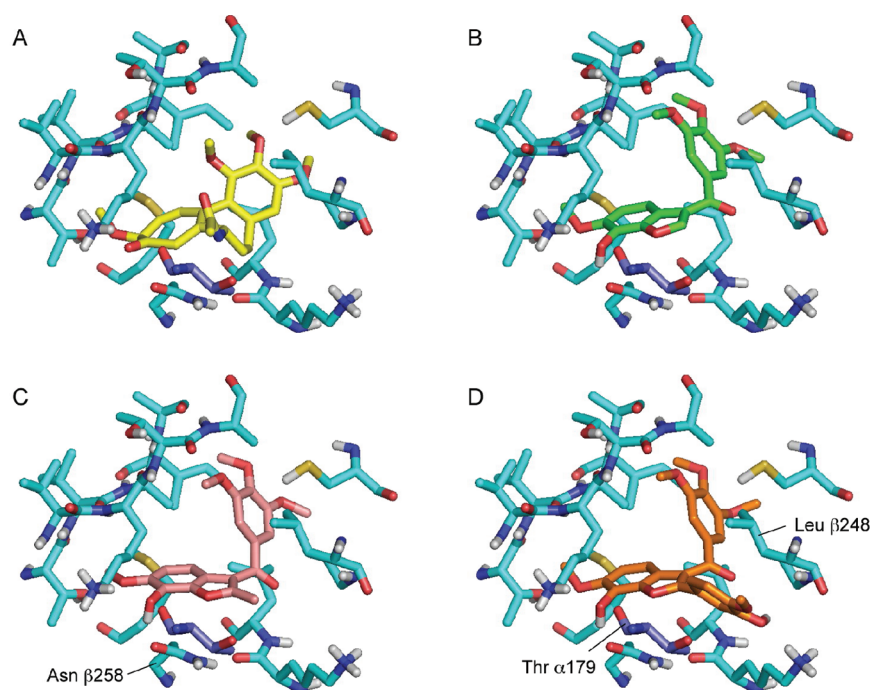
Figure 4. Comparison between the crystal-bound orientation of colchicine (derived from 3E22) (A) and docked orientations of **31b** (B), **8** (C), and **27** (D). The tubulin β subunit is shown with light blue carbon atoms. Residue Thr α179 is shown in dark blue. Note the number scheme used is that described in ref 33.

Table 4. Inhibition of Cell Proliferation by 8 and 4

			8 IC$_{50}$ (nM)	4 IC$_{50}$ (nM)
entry	cell line[a]	cell type		
1	activated HAAE-1	endothelial cell	0.1 (120)[b]	2.2 (1.7)[b]
2	quiescent HAAE-1	endothelial cell	12	1.3
3	U87-MG	brain glioblastoma	0.41	2.6
4	DU145	prostate carcinoma	0.36	4
5	Calu-6	lung anaplastic carcinoma	0.16	0.94
6	MDA-MB-231	breast adenocarcinoma	0.63	3.2
7	A431	epidermoid carcinoma	18.6	188
8	A375	malignant skin melanoma	1.5	2.1
9	SKOV-3	ovary adenocarcinoma	0.59	5.5
10	LoVo	colorectal adenocarcinoma	0.24	2.9
11	AU565	breast adenocarcinoma	5.8	4.4
12	BT549	breast carcinoma	0.34	3.5

[a] HAAE-1 cells were seeded at 500 cells/well in medium containing 0.03 mg/mL endothelial cell growth supplement (activated) or in basal medium containing 0.5% fetal calf serum and antibiotics (quiescent). Cancer cell lines were seeded at an average of 500−2000 cells/well and cultured as recommended by the ATCC. [b] Selectivity ratio (IC$_{50}$ quiescent)/(IC$_{50}$ activated) in parentheses.

Table 5. Effect of MDR-1 Inhibition on the Potency of Antitubulin Drugs toward Renal Carcinoma Cell Line 786-0

	drug IC$_{50}$ (nM) against 786-0 cells			
conditions	paclitaxel	vincristine	vinblastine	8
drug alone	31	37	4.5	0.58
drug + verapamil	4.0	1.2	0.31	0.39

Table 6. Potency of Cytotoxic Drugs toward Resistant Phenotypes of A2780

	drug IC$_{50}$ (nM)		
cell line	doxorubicin	cisplatin	8
A2780	1.2	329	0.03
A2780ADR	194	1103	0.06
A2780cis	5.0	5021	0.01

on tumor growth inhibition, we also observed that **9** is a much more effective inhibitor of tumor growth than **5** (Figure 5). When both compounds were dosed at half their maximum tolerated dose ($^1/_2$ MTD) in a murine breast tumor model,[40] **9** achieved a much greater reduction in tumor growth than did **5** (Figure 5). Furthermore, **9** could achieve a similar reduction in tumor growth at 10 mg/kg ($^1/_8$ MTD) as was achieved by **5** at 150 mg/kg ($^1/_2$ MTD). As previously reported, continued

dosing of **9** at 40 mg/kg ($^1/_2$ MTD) completely suppresses tumor growth and leads to complete eradication of tumors in 14% of the mice after 70 days.[16]

The superior efficacy and therapeutic index of **9**, relative to **5**, can be attributed to a combination of **8**'s greater selectivity, potency, and in vivo exposure. The superior vascular disrupting properties of **9**, relative to **5**, may be derived from **8**'s greater potency and higher free drug fraction. The longer half-life exhibited by **8** (3.5 h), relative to **4** (0.7 h), should enable it to achieve a higher cell kill at the viable rim, as a higher proportion of cells will cycle through the most sensitive phase of the cell cycle (G$_2$-M check point) in the presence of this antimitotic agent.

Table 7. Pharmacokinetic Properties of 4 and 8

	compd[a]	
parameter	4	8
dose (μmol/kg)	6	6
$t_{1/2}$ (h)	0.7	3.5
V_{SS} (L/kg)	7.3	7.1
$AUC_{0-\infty}$	36	48
PPB (% bound)	98.9	81.4

[a] Plasma concentration−time profiles are provided in the Supporting Information.
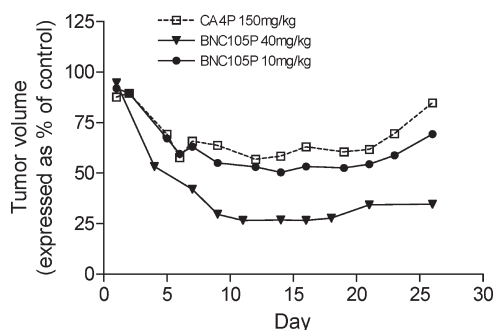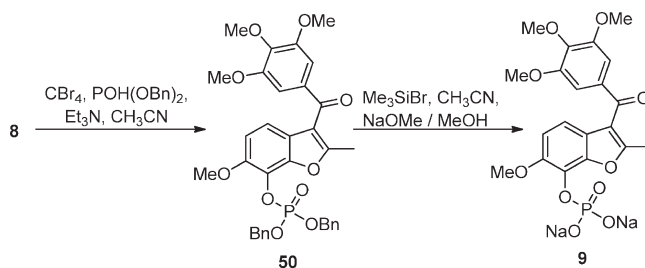
Scheme 2. Synthesis of Prodrug 9

Figure 5. Tumor growth inhibition by **9** and **5** in a MDA-MB-231 breast cancer model: **5** at 150 mg/kg ($^1/_2$ MTD), dosed on days 1 and 5 (□); **9** at 10 mg/kg ($^1/_8$ MTD), dosed days 1 and 5 (●); **9** at 40 mg/kg ($^1/_2$ MTD), dosed days 1 and 8 (▼).

Unlike colchicine, though, **8** is completely cleared from healthy tissues over 24 h, which, in combination with its higher selectivity for activated over quiescent phenotypes, minimizes its toxicity.[16] As previously reported, **8** is trapped in tumor tissue because of the vascular shutdown effect, such that 64% of drug remains in the tumor after 24 h.[16]

■ CONCLUSION

The potency of early leads **I** has been improved by the introduction of a C7-OH. The presence of *both* a C7-OH and a C2-substituent are required for optimal potency. The C2-substituent sterically interacts with the trimethoxybenzoyl unit in **II**, favoring the required cisoid-conformer (cisoid-**II**, Figure 3). The C7-OH group enables an additional hydrogen bonding interaction with Asn β258 to be achieved. Only when both effects are engendered (C7-OH + C2-substituent) is a

significant increase in potency observed (>10 fold). This SAR is maintained across a broad range of C2-subsitutents, and a focused library of potent C2-modified analogues of **II** has been screened for compounds exhibiting selectivity for activated over quiescent endothelial cells. Compound **8** exhibited good selectivity toward activated endothelial cells and was also more potent than **4** against a panel of cancer cell lines. Studies directed toward the molecular basis of this selectivity are ongoing. Compound **8** also exhibited excellent potency against a range of multidrug resistant phenotypes and does not appear to be a substrate for the efflux pump MDR-1. The superior in vivo efficacy of **8**, relative to **4**, is attributed to a combination of its higher potency and greater exposure, enabling it to elicit both vascular disrupting and antimitotic modes of action in vivo. Prodrug **9** is currently undergoing phase II clinical trials for mesothelioma and renal cell carcinoma.[41]

■ EXPERIMENTAL SECTION

Chemistry. Melting points were recorded with an Electrothermal melting point apparatus. Proton (^{1}H) and carbon (^{13}C) NMR spectra were recorded at 300 and 75 MHz, respectively. Liquid chromatography−mass spectrometry (LCMS) was conducted with a C8 column (4.6 mm × 150 mm), using an isocratic mobile-phase containing 49% acetonitrile, 50% and 315 water, and a 1% ammonium formate solution (this solution was made up of 1 g of acetic acid and 315 mg of ammonium formate in 1 L of 33% methanol in water) at a constant flow rate of 0.5 mL/min. UV detection was measured at 214 nm, and MS analysis was conducted using an atmospheric pressure ionization (APCI) ion source. High-resolution mass spectrometry (HRMS) was performed on a time-of-flight mass spectrometer fitted with an electrospray (ESI) ion source. Tetrahydrofuran (THF) and diethyl ether were distilled under nitrogen from sodium benzophenone ketyl. Dichloromethane and 1,2-dichloroethane were distilled from calcium hydride under nitrogen. Analytical thin layer chromatography (TLC) was conducted on aluminum sheets coated with silica gel 60 GF254. Flash chromatography was performed on flash grade silica gel. Experimental methods for the following compounds has been previously reported: **8**, **16a**, **16b**, **30a**, **30b**, **31a**, **32**, **33a**, **33b**, **35**, **36**, **44**, **47**.[24] All test compounds (Table 3) exhibited >95% purity by LCMS except **26**, which was 91% pure by LCMS.

General Procedure A: Multicomponent Coupling of 16, 17, and 19. To a solution of 2-iodophenol **16** (1 mmol) and alkyne (1.2 mmol) in dry THF (5 mL) under nitrogen at 0 °C was added MeMgCl (3.0 M solution in THF, 2.5 mmol), and the mixture was allowed to warm to room temperature. Pd(Ph₃P)₂Cl (3 mol %) was added and the mixture heated to 65 °C for 4−8 h (monitoring by TLC). The reaction mixture was then cooled to room temperature and the THF removed under vacuum. Aryl iodide **19** (1.1 mmol) was added, and the mixture was dissolved in DMSO (12 mL/mmol). The nitrogen atmosphere was replaced with carbon monoxide (balloon). The aryl iodide (1.05 mmol) was added, and the mixture was heated to 80 °C overnight, then quenched with 10% NH₄Cl (aq) and extracted with ethyl acetate. The organic layer was washed with brine and the solvent removed under vacuum. The residue was concentrated onto silica gel and purified by flash column chromatography.

2-(3-*N*,*N*-Dibenzyl-4-methoxy-phenyl)-6-methoxy-3-(3,4,5-trimethoxybenzoyl)benzo[*b*]furan 20. 20 was prepared from **16a**, **17a**, and **19** in accordance with general procedure A. Flash chromatography: silica gel, eluent = hexane/diethyl ether 8:2, yield 31%. ^{1}H NMR (300 MHz, CDCl₃) δ 7.50 (d, *J* = 8.71 Hz, 1H), 7.27−7.05 (m, 16H), 6.88 (dd, *J* = 8.68, 2.23 Hz, 1H), 4.03 (br s, 4H), 3.87 (s, 6H), 3.80 (s, 3H), 3.58 (s, 6H).

6-Methoxy-2-(N-methyl-5-indolyl)-3-(3,4,5-trimethoxybenzoyl)benzo[b]furan 21. 21 was prepared from 16a, 17b, and 19 in accordance with general procedure A. Flash chromatography: silica gel, eluent = hexane/diethyl ether 8:2, yield 32%. ^{1}H NMR (300 MHz, CDCl$_3$) δ 7.91 (d, J = 1.19 Hz, 1H), 7.60 (d, J = 8.65 Hz, 1H), 7.32−7.36 (m, 2H), 7.14 (d, J = 8.63 Hz, 1H), 7.11 (s, 2H), 7.01 (d, J = 3.11 Hz, 1H), 6.92 (dd, J = 9.95, 2.27 Hz, 1H), 6.41 (d, J = 3.08 Hz, 1H) 3.89 (s, 6H), 3.76 (s, 3H), 3.74 (s, 3H), 3.61 (s, 3H). ^{13}C NMR (75 MHz, CDCl$_3$) δ 191.0, 159.1, 158.0, 154.5, 152.4, 141.7, 136.7, 132.6, 129.6, 127.9, 122.0, 121.9, 121.27, 120.8, 113.9, 112.1, 108.7, 107.05, 101.6, 95.4, 60.4, 55.6, 55.4, 32.5. LCMS: t_R = 2.71 min, >99%. MS m/z = 472 (M + H)$^+$, 100%. HRMS: calcd for C$_{28}$H$_{26}$NO$_6^+$ = 472.1760, found = 472.1761.

2-(4-Benzyloxyphenyl)-6-methoxy-3-(3,4,5-trimethoxybenzoyl)benzo[b]furan 22. 22 was prepared from 16a, 17c, and 19 in accordance with general procedure A. Flash chromatography: silica gel, eluent = hexane/diethyl ether, 8:2 and then 7:3, yield 29%. ^{1}H NMR (300 MHz, CDCl$_3$) δ 7.54 (d, J = 8.96 Hz, 2H), 7.49 (d, J = 8.67 Hz, 1H), 7.36−7.38 (m, 5H), 7.11 (s, 2H), 7.07 (d, J = 2.19 Hz, 1H), 6.90 (dd, J = 8.60, 2.20 Hz, 1H), 6.86 (d, J = 8.92 Hz, 2H), 5.04 (br s, 2H) 3.87 (s, 3H), 3.86 (s, 3H), 3.67 (s, 6H).

7-Isopropoxy-2-(3-isopropoxy-4-methoxyphenyl)-6-methoxy-3-(3,4,5-trimethoxybenzoyl)benzo[b]furan benzo[b]furan 23. 23 was prepared from 16b, 17d, and 19 in accordance with general procedure A. Flash chromatography: silica gel, eluent = hexane/diethyl ether, 8:2 and then 7:3, yield 46%. ^{1}H NMR (300 MHz, CDCl$_3$) δ 7.26 (d, J = 8.58 Hz, 1H), 7.18 (dd, J = 8.44, 2.14 Hz, 1H), 7.13 (s, 2H), 7.07 (d, J = 2.02 Hz, 1H), 6.93 (d, J = 8.65 Hz, 1H), 6.81 (d, J = 8.52 Hz, 1H), 4.77 (quintet, 1H), 4.22 (quintet, 1H), 3.91 (s, 3H), 3.85 (s, 3H), 3.83 (s, 3H), 3.68 (s, 6H), 1.42 (d, J = 6.17 Hz, 6H), 1.23 (d, J = 6.17 Hz, 6H).

7-Isopropoxy-6-methoxy-2-(4-N-methylpyrazolyl)-3-(3,4,5-trimethoxybenzoyl)benzo[b]furan 24. 24 was prepared from 16b, 17f, and 19 in accordance with general procedure A. Flash chromatography: silica gel, eluent = hexane/diethyl ether, 8:2 and then 7:3, yield 55%. ^{1}H NMR (300 MHz, CDCl$_3$) δ 8.12 (s, 1H), 7.98 (s, 1H), 7.13 (s, 2H), 6.84 (d, J = 8.63 Hz, 1H), 6.79 (d, J = 8.67 Hz, 1H), 4.73 (quintet, 1H), 3.93 (br s, 6H), 3.88 (s, 3H), 3.77 (s, 6H), 1.41 (d, J = 6.16 Hz, 6H). LCMS: t_R = 2.27 min, >99%. MS m/z = 481 (M + H)$^+$, 100%. HRMS: calcd for C$_{24}$H$_{26}$NO$_7^+$ = 481.1975, found = 481.1974.

2-(3-Amino-4-methoxyphenyl)-6-methoxy-3-(3,4,5-trimethoxybenzoyl)benzo[b]furan 25. Catalyst 10% Pd/C (60 mg) was added to a solution of 20 (60 mg, 0.093 mmol) in ethyl acetate (12 mL), methanol (5 mL), and water (2.5 mL), followed by 1 drop of HCl (aq) (6 M), and the reaction mixture was stirred under an atmosphere of hydrogen (balloon) for 1 h. The mixture was filtered through Celite and washed with dichloromethane (2 × 5 mL) and the solvent removed under vacuum. The crude product was purified by preparative layer chromatography (eluent = hexane/ethyl acetate/triethylamine 6:4:1) to give a yellow paste that was recrystallized from hexane and dichloromethane (vapor diffusion) to afford 25 as a yellow solid (14.7 mg, 34%). ^{1}H NMR (300 MHz, CDCl$_3$) δ 7.47 (d, J = 8.64 Hz, 1H), 7.12 (s, 2H), 7.09−7.05 (m, 2H), 6.99 (dd, J = 8.39, 1.57 Hz, 1H), 6.88 (dd, J = 8.41, 2.18 Hz, 1H), 6.65 (d, J = 8.38 Hz, 1H), 6.31 (br s, 2H), 3.86 (br s, 6H), 3.81 (s, 3H), 3.70 (s, 6H). ^{13}C NMR (75 MHz, CDCl$_3$) δ 190.7, 158.1, 157.0, 154.2, 152.5, 148.4, 142.0, 134.7, 132.4, 122.3, 121.7, 121.3, 119.9, 114.4, 114.3, 112.2, 109.6, 107.0, 95.3, 60.6, 55.8, 55.4, 55.2. LCMS: t_R = 2.14 min, >99%. MS m/z = 464 (M + H)$^+$, 100%. HRMS: calcd for C$_{26}$H$_{26}$NO$_7^+$ = 464.1709, found = 464.1707.

2-(4-Hydroxyphenyl)-6-methoxy-3-(3,4,5-trimethoxybenzoyl)benzo[b]furan 26. A mixture of 30 (45 mg, 0.09 mmol) and Pd/C (10%, 40 mg) in a mixture of ethyl acetate (7 mL) and triethylamine (3 drops) was stirred under an atmosphere of hydrogen for 1 h. The mixture was filtered through Celite and washed with

dichloromethane (2 × 5 mL), and the solvent was removed under vacuum. Purification by flash chromatography (silica gel, eluent = hexane/ethyl acetate, 6:4) gave a yellow paste that was recrystallized from hexane and dichloromethane (vapor diffusion) to afford 26 as a yellow solid (23.2 mg, 63%). ^{1}H NMR (300 MHz, CDCl$_3$) δ 7.49 (dd, 2 × J = 8.36 Hz, 3H), 7.11 (s, 2H), 7.07 (d, J = 2.06 Hz, 1H), 6.89 (dd, J = 8.62, 2.18 Hz, 1H), 6.74 (d, J = 8.69 Hz, 2H), 3.87 (s, 3H), 3.86 (s, 3H), 3.69 (s, 6H). ^{13}C NMR (75 MHz, CDCl$_3$) δ 191.0, 158.1, 157.4, 157.2, 154.3, 152.5, 142.2, 132.3, 129.7, 127.1, 121.7, 121.3, 115.2, 114.1, 112.3, 107.3, 95.4, 60.6, 55.8, 55.4. LCMS: t_R = 2.38 min, >90%. MS m/z = 435 (M + H)$^+$, 38%; 157, 100%. HRMS: calcd for C$_{25}$H$_{23}$NO$_7^+$ = 435.1444, found = 435.1442.

7-Hydroxy-2-(3-hydroxy-4-methoxyphenyl)-6-methoxy-3-(3,4,5-trimethoxybenzoyl)benzo[b]furan 27. To a solution of 23 (62 mg, 0.11 mmol) in dry dichloromethane (3 mL) was added AlCl$_3$ (37 mg, 0.28 mmol). The reaction mixture was stirred vigorously at room temperature for 5 h. Another portion of AlCl$_3$ (18 mg, 0.14 mmol) was added, and stirring continued for 20 min (TLC). The reaction was quenched with saturated NH$_4$Cl (aq), and the aqueous layer was extracted with ethyl acetate (20 mL). The organic layer was washed with water (15 mL), dried over MgSO$_4$, and concentrated under vacuum. The crude product was purified by flash chromatography (silica gel, gradient elution = hexane/diethyl ether 2:8, then neat diethyl ether) to afford 27 as a crystalline yellow solid (27 mg, 51%). ^{1}H NMR (300 MHz, CDCl$_3$) δ 7.25 (d, J = 2.34 Hz, 1H), 7.12 (d, J = 8.92 Hz, 1H), 7.10 (dd, J = 8.36, 2.14 Hz, 1H), 7.10 (s, 2H), 6.91 (d, J = 8.59 Hz, 1H), 6.70 (d, J = 8.45 Hz, 1H), 5.71 (br s, 1H), 5.52 (br s, 1H), 3.96 (s, 3H), 3.86 (s, 3H), 3.85 (s, 3H), 3.69 (s, 6H). LCMS: t_R = 1.62 min, >99%. MS m/z = 481 (M + H)$^+$, 100%. HRMS: calcd for C$_{26}$H$_{24}$O$_9^+$ = 481.1499, found = 481.1501.

7-Hydroxy-6-methoxy-2-(4-N-methylpyrazolyl)-3-(3,4,5-trimethoxybenzoyl)benzo[b]furan 28. To a solution of 24 (85 mg, 0.18 mmol) in dry dichloromethane (3 mL) was added AlCl$_3$ (48 mg, 0.36 mmol). The reaction mixture was stirred vigorously at room temperature for 10 min. Another portion of AlCl$_3$ (10 mg, 0.08 mmol) was added, and stirring continued for 20 min (TLC). The reaction was quenched with saturated NH$_4$Cl (aq), and the aqueous layer was extracted with ethyl acetate (20 mL). The organic layer was washed with water (15 mL), dried over MgSO$_4$, and concentrated under vacuum. The crude product was purified by flash chromatography (silica gel, gradient elution = hexane/diethyl ether 2:8, then neat diethyl ether) to afford the title compound as a crystalline yellow solid (58 mg, 75%). ^{1}H NMR (300 MHz, CDCl$_3$) δ 8.15 (s, 1H), 8.03 (s, 1H), 7.13 (s, 2H), 6.79 (d, J = 8.62 Hz, 1H), 6.69 (d, J = 8.58 Hz, 1H), 3.92 (br s, 6H), 3.91 (s, 3H), 3.77 (s, 6H). LCMS: t_R = 1.63 min, >99%. MS m/z = 439 (M + H)$^+$, 100%. HRMS: calcd for C$_{23}$H$_{22}$NO$_7^+$ = 439.1505, found = 439.1510.

7-Hydroxy-6-methoxy-3-(3,4,5-trimethoxybenzoyl)benzo[b]furan 31b. *Step 1.* Tetrabutylammonium fluoride (76.5 μL, 0.076 mmol, 1 M solution in THF) was added to a stirred solution of 30b^{24} (0.066 mmol) in THF (1 mL). The reaction mixture was stirred at room temperature for 20 min (TLC), diluted with ethyl acetate (10 mL), and washed with 1 M HCl (5 mL). The organic layer was dried over MgSO$_4$, and the solvent was removed under vacuum. The crude product was purified by flash chromatography (silica gel, eluent = hexane/diethyl ether, 7:3) to afford the 3-(3,4,5-trimethoxybenzoyl)-6-methoxy-7-isopropoxybenzo[b]furan as a light yellow paste (23 mg) that was used directly in the next step. ^{1}H NMR (300 MHz, CDCl$_3$) δ 8.00 (s, 1H), 7.78 (d, J = 8.60 Hz, 1H), 7.15 (s, 2H), 7.04 (d, J = 8.61 Hz, 1H), 4.73 (m, 1H), 3.93 (s, 3H), 3.92 (s, 3H), 3.90 (s, 6H), 1.37 (d, J = 6.14 Hz, 6H).

Step 2. A solution of the product from step 1 (23 mg, 0.058 mmol) in dry dichloromethane (1 mL) was treated with AlCl$_3$ (16 mg, 0.116 mmol). The reaction mixture was stirred for 0.5 h at room temperature, then quenched with saturated NH$_4$Cl (aq) and extracted with ethyl acetate (10 mL). The organic layer was washed with water (5 mL), dried over MgSO$_4$ and concentrated under vacuum. The crude product was

purified by flash chromatography (silica gel, eluent = hexane/diethyl ether/ethyl acetate, 80:20:1) to afford **31b** as a cream crystalline solid (18 mg, 86%). ^{1}H NMR (300 MHz, CDCl$_3$) δ 8.04 (s, 1H), 7.63 (d, J = 8.53 Hz, 1H), 7.14 (s, 2H), 7.02 (d, J = 8.38 Hz, 1H), 5.69 (s, 1H), 3.97 (s, 3H), 3.93 (s, 3H), 3.89 (s, 6H). ^{13}C NMR (75 MHz, CDCl$_3$) δ 188.7, 152.8, 151.2, 144.5, 143.3, 141.8, 134.0, 130.9, 120.92, 120.6, 112.4, 109.2, 106.1, 60.6, 56.9, 56.0. LCMS: t_R = 1.73 min, >99%. MS m/z = 359 (M + H)$^+$, 100%. HRMS: calcd for C$_{19}$H$_{19}$O$_7^+$ = 359.1131, found = 359.1126.

(*E*)-3-(7-Hydroxy-6-methoxy-3-(3,4,5-trimethoxybenzoyl)-benzofuran-2-yl)acrylamide 40. Pd(OAc)$_2$ (5.0 mg, 0.02 mmol) was added to a solution of **33b** (48 mg, 0.10 mmol) and acrylamide **38b** (70 mg, 1 mmol) in a mixture of acetonitrile and triethylamine (2:1, 1.5 mL) and the resulting solution degassed (stirring solution exposed to a partial vacuum and backfilled with N$_2$ gas 3 times). The reaction mixture was stirred at reflux for 1 h. More palladium acetate (5.0 mg, 0.02 mmol) was added, and refluxing continued for 7 h (monitored by TLC). The solvent was removed under vacuum and the residue subjected to flash chromatography (silica gel, eluent = hexane/diethyl ether 1:1) affording the title compound **40** as a yellow crystalline solid (7.3 mg, 17%). ^{1}H NMR (300 MHz, CD$_3$OD) δ: 7.48 (d, J = 15.5 Hz, 1H), 7.18 (s, 2H), 7.00 (d, J = 8.65 Hz, 1H), 6.94 (d, J = 15.5 Hz, 1H), 6.88 (d, J = 8.62 Hz, 1H), 5.46 (s, 1H), 4.55 (br s, 2H), 3.91 (s, 3H), 3.87 (s, 3H), 3.79 (s, 6H). LCMS: t_R = 1.49 min, >99%. MS m/z = 424 (M + H)$^+$, 100%. HRMS: calcd for C$_{22}$H$_{22}$NO$_8^+$ = 428.1345, found = 428.1345.

2-(2,3-Dihydro-1*H*-pyrrol-1-yl)-7-hydroxy-6-methoxy-3-(3,4,5-trimethoxybenzoyl)benzo[*b*]furan 42. To a solution of pyrrole (22 mg, 0.32 mmol) in dry THF (2 mL) was added sodium hydride (60%, 24 mg, 0.60 mmol), and the resulting suspension was stirred at room temperature for 24 h. To this solution **33b** (50 mg, 0.10 mmol) was added, and the reaction mixture was stirred at room temperature for 18 h (monitored by TLC), quenched with saturated NH$_4$Cl (aq) (10% w/v, 3 mL), extracted with dichloromethane (10 mL), dried over MgSO$_4$, and concentrated under vacuum. The resultant residue was purified by planar chromatography on silica gel (eluent = hexane/ethyl acetate 3:1) to give the title compound **42** as a yellow solid (25 mg, 60%). ^{1}H NMR (300 MHz, CDCl$_3$) δ 8.47 (d, J = 1.21 Hz, 1H), 7.75 (d, J = 1.20 Hz, 1H), 7.27 (d, J = 8.60 Hz, 1H), 7.18 (d, J = 8.66 Hz, 1H), 7.05 (s, 2H), 6.17 (t, J = 2.3 Hz, 2H), 5.27 (s, 1H), 3.94 (s, 3H), 3.74 (s, 6H), 3.73 (s, 3H). LCMS: t_R = 1.77 min, >99%. MS m/z = 424 (M + H)$^+$, 100%. HRMS: calcd for C$_{23}$H$_{22}$NO$_7^+$ = 424.1396, found = 424.1396.

6-Methoxy-2-(4-*N*-methylpiperazino)-3-(3,4,5-trimethoxy-benzoyl)benzo[*b*]furan 45. *N*-Methylpiperazine (50 μL, 0.45 mmol) was added to a stirred solution of **33a** (17 mg, 0.041 mmol) in acetonitrile/dichloromethane 1:1 (2 mL), and the reaction mixture was stirred at room temperature for 1 h. After this time the solvent was removed under vacuum, and the resultant residue was purified by planar chromatography on silica gel (eluent, hexane/ethyl acetate 4:6 + 1% triethylamine) to give the title compound as a yellow paste (8 mg, 43%). ^{1}H NMR (300 MHz, CDCl$_3$) δ 7.07 (s, 2H), 6.93 (d, J = 8.60 Hz, 1H), 6.84 (d, J = 2.25 Hz, 1H), 6.65 (dd, J = 8.64, 2.30 Hz, 1H), 3.92 (s, 3H), 3.83 (s, 6H), 3.78 (s, 3H), 3.66−3.64 (m, 4H), 2.65−2.63 (m, 4H), 2.40 (s, 3H). ^{13}C NMR (75 MHz, CDCl$_3$) δ 188.8, 162.2, 155.9, 152.7, 149.1, 141.1, 135.4, 121.7, 119.64, 110.4, 106.1, 155.9, 95.6, 60.6, 55.9, 55.4, 53.9, 47.1, 45.3. LCMS: t_R = 1.78 min, >99%. MS m/z = 441 (M + H)$^+$, 100%. HRMS: calcd for C$_{24}$H$_{29}$N$_2$O$_6^+$ = 441.2026, found = 441.2030.

2-(2-Dimethylaminoethylamino)-7-hydroxy-6-methoxy-3-(3,4,5-trimethoxybenzoyl)benzo[*b*]furan 46. *N,N*-Dimethyl-ethylenediamine (500 μL) was added to a stirred solution of **33b** (50 mg, 0.10 mmol) in dry pyridine (2 mL) and the reaction mixture stirred at 80 °C for 1 h. The reaction mixture was cooled to room temperature, concentrated under vacuum and the residue purified by flash chromatography (silica gel, eluent hexane/ethyl acetate 4:1 with

1% triethylamine), affording the title compound as light yellow solid (25 mg, 54%). ^{1}H NMR (300 MHz, CDCl$_3$) δ 9.10 (br s, 1H), 6.95 (s, 2H), 6.60 (d, J = 8.44 Hz, 1H), 6.48 (d, J = 8.48 Hz, 1H), 3.90 (s, 3H), 3.84 (s, 3H), 3.83 (s, 6H), 3.82 − 3.83 (m, 2H), 2.65 (t, J = 5.63 Hz, 2H), 2.34 (s, 6H). LCMS: t_R = 1.65 min, >99%. MS m/z = 445 (M + H)$^+$, 100%. HRMS: calcd for C$_{23}$H$_{29}$N$_2$O$_7^+$ = 445.1975, found = 445.1978.

2-Benzylamino-7-hydroxy-6-methoxy-3-(3,4,5-trimethoxy-benzoyl)benzo[*b*]furan 48. When the reaction above was performed using benzylamine in the place of *N,N*-dimethylethylenedia-mine, product **48** was obtained as a light yellow solid (112 mg, 83%). ^{1}H NMR (300 MHz, CDCl$_3$) δ 9.27 (bs, NH, 1H), 7.39−7.32 (m, 5H), 6.96 (s, 2H), 6.61 (d, J = 8.47 Hz, 1H), 6.50 (d, J = 8.10 Hz, 1H,), 4.83 (d, J = 4.95 Hz, 2H), 3.91 (s, 3H), 3.85 (s, 3H), 3.84 (s, 6H).

2-Amino-7-hydroxy-6-methoxy-3-(3,4,5-trimethoxyben-zoyl)benzo[*b*]furan 49. 10% Pd/C (100 mg) was added to a solution of **48** (105 mg, 0.23 mmol) in a mixture of ethyl acetate/THF/water 3:2:1 (6 mL), and 2 drops of HCl (aq) (6 M) were added. The resultant mixture was stirred at room temperature for 2.5 h under H$_2$ (g) (balloon). After this time, the mixture was filtered through Celite, the filtrate diluted with water (10 mL) and extracted with dichloromethane (5 mL × 3). The organic phase was dried over MgSO$_4$ and concentrated under vacuum. The resultant residue was purified by flash chromatography (silica gel, eluent hexane/ethylacetate 4:1) to give **49** as a crystalline yellow solid (79 mg, 93%). ^{1}H NMR (300 MHz, CDCl$_3$) δ 6.98 (s, 2H), 6.93 (br s, 2H), 6.63 (d, J = 8.18 Hz, 1H), 6.52 (d, J = 8.41 Hz, 1H), 5.65 (br s, 1H), 3.92 (s, 3H), 3.86 (s, 3H), 3.84 (s, 6H). LCMS: t_R = 1.628 min, >99%. MS m/z = 374 (M + H)$^+$, 100%. HRMS: calcd for C$_{19}$H$_{20}$NO$_7^+$ = 374.1240, found = 374.1237.

Dibenzyl (6-Methoxy-2-methyl-3-(3,4,5-trimethoxyben-zoyl)benzofuran-7-yl)phosphate 50. Triethylamine (0.295 mL, 2.12 mmol) was added dropwise with stirring to a suspension of **8** (0.36 g, 0.97 mmol), CBr$_4$ (0.383 g, 1.15 mmol), and dibenzyl phosphite (0.28 mL, 1.27 mmol) in anhydrous acetonitrile (5 mL) at 0 °C under a N$_2$ (g) atmosphere. The resulting homogeneous mixture was stirred for 2 h at room temperature and evaporated to dryness under reduced pressure. The residue was diluted to 40 mL with ethyl acetate, washed with 0.1 M HCl (10 mL), water (10 mL), brine (10 mL), and dried over anhydrous MgSO$_4$. Filtration and evaporation of the filtrate under reduced pressure gave 0.68 g of crude product, which was purified by flash column chromatography (silica gel, hexane/ethyl acetate 7:3) to give of **50** as a cream solid (0.455 g, 74%). ^{1}H NMR (300 MHz, CDCl$_3$) δ 7.3−7.43 (m, 10H), 7.21 (d, J = 8.7 Hz, 1H), 7.08 (s, 2H, CH), 6.89 (d, J = 8.7 Hz, 1H), 5.32 (m, 4H,), 3.93 (s, 3H), 3.83 (s, 9H), 2.42 (s, 3H).

Disodium (6-Methoxy-2-methyl-3-(3,4,5-trimethoxyben-zoyl)benzofuran-7-yl)phosphate 9. Bromotrimethylsilane (0.3 mL) was added dropwise to a stirred solution of **50** (0.455 g, 0.719 mmol) in anhydrous acetonitrile (5 mL) at −5 °C under a N$_2$ (g) atmosphere. The reaction mixture was allowed to warm to 0 °C over 1 h, then evaporated to dryness under reduced pressure. The residue was dissolved in 90% aqueous acetonitrile (15 mL) and evaporated to dryness. The crystalline residue was washed with a 50% hexane/dichloromethane mixture (20 mL) to give the free acid of **9** (0.302 g, 93%). This was suspended in anhydrous methanol (15 mL), and a solution of MeONa (0.073 g, 1.34 mmol) in methanol (1 mL) was added, with stirring, at room temperature. The pH of the resulting mixture was further adjusted to 10 by addition of a small amount of additional MeONa, and the mixture was evaporated to dryness. The residue was dissolved in water (2 mL), and acetonitrile (10 mL) was added. The product crystallized, was removed by filtration, rinsed with cold (0 °C) acetonitrile (5 mL) and diethyl ether (10 mL), and air-dried for 24 h to a constant mass to give pure **9** (tetrahydrate) as a creamy solid (0.33 g, 92%). ^{1}H NMR (300 MHz, D$_2$O) δ 7.10 (s, 2H),

7.04 (d, J = 8.6 Hz, 1H), 6.94 (d, J = 8.6 Hz, 1H), 2.37 (s, 3H), 3.76 (s, 6H), 3.79 (s, 3H), 3.81 (s, 3H), 4.66 (s, hydrate, 8H). LCMS, t_R = 1.16, >99%. MS m/z = 452.8 (M − 2Na + 3H), 100%. HRMS: calcd for $C_{20}H_{20}O_{10}P^-$ = 451.0794, found = 451.0769.

Docking. Molecular docking was performed with Glide 5.6 (Schrödinger LLC) using XP mode with default settings. Ligands were prepared using LigPrep, version 2.4. Default settings were used, unless stated otherwise. Compounds were docked into the crystal structure of the colchicine binding site of the bovine tubulin/stathmin complex (PDB entry 1SA1) which contains a podophylotoxin ligand.[33]

Biology. The following assays were run according to previously described methods: tubulin polymerization assay[42] and MCF-7 proliferation assay.[43]

Cell Culture and Cell Lines. All in vitro assays were carried out using endothelial cells derived from human umbilical vein (HUVEC) (Clonetics Lonza, Walkersville, MD, U.S.) or human abdominal aorta (HAAE-1) (ATCC, Manassas, VA, U.S.). HUVEC were routinely cultured in EGM-2 medium (Clonetics), and HAAE-1 cells were cultured in F12K medium (Gibco, Invitrogen, Auckland, NZ) containing 10% fetal calf serum, 0.1 mg/mL heparin (Sigma-Aldrich, St. Louis, MO, U.S.), 0.03 mg/mL endothelial cell growth supplement (Sigma-Aldrich, St. Louis, MO, U.S.), 2 mM penicillin−streptomycin−glutamine (Gibco, Invitrogen, Auckland, NZ), and 10 mM Hepes buffered solution (Gibco, Invitrogen, Auckland, NZ). Endothelial cell cultures between passages 2 and 6 were used for all assays. Cancer cell lines were obtained from ATCC (Manassas, VA, U.S.) and cultured as recommended by the supplier. All cells were cultured in a humidified incubator at 37 °C with 5% CO_2.

Endothelial Cell Proliferation Assay. HUVEC or HAAE-1 cell cultures were exposed to a concentration range of 0.1−1000 nM for each test compound tested. Proliferation assays were carried out in triplicate in 96-well plates. For activated growth conditions HUVEC and HAAE-1 cells were seeded at 2500 and 500 cells/well, respectively, and cultured in EBM-2 or F12K medium containing 0.03 mg/mL endothelial cell growth supplement (Sigma-Aldrich, St. Louis, MO, U.S.) as described above. For quiescent growth conditions HUVEC and HAAE-1 cells were seeded at 15 000 and 5000 cells/well, respectively, in basal medium (EBM-2 or F12K) containing 0.5% fetal calf serum and antibiotics. Cancer cell lines were seeded at an average of 500−2000 cells/well. Cells were allowed to adhere overnight, followed by incubation with compounds under evaluation for 48−72 h. Metabolically active cells were measured using CellTiter 96 Aqueous One Solution (Promega Corp., Madison WI, U.S.) according to the manufacturer's instructions, and absorbance readings were taken at 492 nm. Absorbance readings for each compound concentration were normalized to corresponding vehicle control cultures. A sigmoidal dose−response curve was fitted to the data, and the concentration at which proliferation decreased by 50% was calculated using Graph Pad Prism 4 software (San Diego, CA, U.S.).

ASSOCIATED CONTENT

ⓢ Supporting Information. Complete listing of benzo-[*b*]furan compounds tested; synthesis of **17a**, **17b**, and **17f**; results of pharmacokinetic studies of **4**, **5**, **8**, and **9**. This material is available free of charge via the Internet at http://pubs.acs.org.

AUTHOR INFORMATION

Corresponding Author
*Phone: +61 399039650. Fax: +61 99039143. E-mail: bernard.flynn@monash.edu.

ABBREVIATIONS USED

CA4, combretastatin A-4; CA4P, combretastatin A-4 disodium phosphate; HUVEC, human umbilical vein endothelial cell; HAEEC, human aortic arterial endothelial cell; IC_{50}, inhibitory concentration 50%; LD_{50}, lethal dose 50%; MCC, multicomponent coupling; MDR, multidrug resistance; MTD, maximum tolerated dose; SAR, structure−activity relationship; VDA, vascular disrupting agent

REFERENCES

(1) (a) Jordan, M. A.; Wilson, L. Microtubules as a target for anticancer drugs. *Nat. Rev. Cancer* **2004**, *4*, 253–265. (b) Lopus, M.; Yenjerle, M.; Wilson, L. Microtubule Dynamics. In *Wiley Encyclopedia of Chemical Biology*; Begley, T. P., ; Eds.; John Wiley and Sons, Inc.: Hoboken, NJ, 2008; 3, 153−160. (c) Etienne-Manneville, S. From signaling pathways to microtubule dynamics: the key players. *Curr. Opin. Cell Biol.* **2010**, *22*, 104–111. (d) Wade, R. H. On and around microtubules: an overview. *Mol. Biotechnol.* **2009**, *43*, 177–191.

(2) (a) Kavallaris, M.; Verrills, N. M.; Hill, B. T. Anticancer therapy with novel tubulin-interacting drugs. *Drug Resist. Updates* **2001**, *4*, 392–401. (b) Hearn, B. R.; Shaw, S. J.; Myles, D. C. *Microtubule Targeting Agents, Compr. Med. Chem. II* **2006**, *7*, 81–110. (c) Bedard, P. L.; Di Leo, A.; Piccart-Gebhart, M. J. Taxanes: optimizing adjuvant chemotherapy for early-stage breast cancer. *Nat. Rev. Clin. Oncol* **2010**, *7*, 22–36. (d) Hadfield, J. A.; Ducki, S.; Hirst, N.; McGown, A. T. Tubulin and microtubules as targets for anticancer drugs. *Prog. Cell Cycle Res.* **2003**, *5*, 309–325.

(3) Recent reviews: (a) Chen, J.; Liu., T.; Dong, X.; Hu, Y. Recent developments and SAR analysis of colchicine binding site inhibitors. *Mini-Rev. Med. Chem.* **2009**, *9*, 1174–1190. (b) Chaudhary, A.; Pandeya, S. N.; Kumar, P.; Sharma, P. P.; Gupta, S.; Soni, N.; Verma, K. K.; Bhardwaj, G. Combretastatin A-4 analogs as anticancer agents. *Mini-Rev. Med. Chem.* **2007**, *7*, 1186–1205. (c) Tron, G. C.; Pirali, T.; Sorba, G.; Pagliai, F.; Busacca, S.; Genazzani, A. A. Medicinal chemistry of combretastatin A4: present and future directions. *J. Med. Chem.* **2006**, *49*, 3033–3044. (d) Pinney, K. G.; Jelinek, C.; Edvardsen, K.; Chaplin, D. J.; Pettit, G. R. The Discovery and Development of the Combretastatins. In *Anticancer Agents from Natural Products*; Cragg, G. M., Kingston, D. G. I., Newman, D. J., Eds; Taylor and Francis: Boca Raton, FL, 2005; pp 23−46. (e) Bhattacharyya, B.; Panda, D.; Gupta, S.; Banerjee, M. Antimitotic activity of colchicine and the structural basis for its interaction with tubulin. *Med. Res. Rev.* **2008**, *28*, 155–183. (f) Hamel, E. An Overview of Compounds That Interact with Tubulin and Their Effects on Microtubule Assembly. In *The Role of Microtubules in Cell Biology, Neurobiology and Oncology*; Fojo, T., Ed.; Humana Press: Totowa, NJ, 2008; pp 1−19.

(4) (a) Romagnoli, R.; Baraldi, P. G.; Carrion, M. D.; Cruz-Lopez, O.; Tolomeo, M.; Grimaudo, S.; Di Cristina, A.; Pipitone, M. R.; Balzarini, J.; Brancale, A.; Hamel, E. Substituted 2-(3′,4′,5′-trimethoxybenzoyl)-benzo[*b*]thiophene derivatives as potent tubulin polymerization inhibitors. *Bioorg. Med. Chem.* **2010**, *18*, 5114–5122. (b) Chen, J.; Wang, Z.; Lu, Y.; Dalton, J. T.; Miller, D. D.; Li, W. Synthesis and antiproliferative activity of imidazole and imidazoline analogs for melanoma. *Bioorg. Med. Chem. Lett.* **2008**, *18*, 3183–3187. (c) Lu, Y.; Li, C. M.; Wang, Z.; Ross, C. R., II; Chen, J.; Dalton, J. T.; Li, W.; Miller, D. D. Discovery of 4-substituted methoxybenzoyl-aryl-thiazoles as novel anticancer agents: synthesis, biological evaluation, and structure−activity relationships. *J. Med. Chem.* **2009**, *52*, 1701–1711. (d) La Regina, G.; Sarkar, T.; Bai, R.; Edler, M. C.; Saletti, R.; Coluccia, A.; Piscitelli, F.; Minelli, L.; Gatti, V.; Mazzoccoli, C.; Palermo, V.; Mazzoni, C.; Falcone, C.; Scovassi, A. I.; Giansanti, V.; Campiglia, P.; Porta, A.; Maresca, B.; Hamel, E.; Brancale, A.; Novellino, E.; Silvestri, R. New arylthioindoles and related bioisosteres at the sulfur bridging group. 4. Synthesis, tubulin polymerization, cell growth inhibition, and molecular modeling studies. *J. Med. Chem.* **2009**, *52*, 7512–7527. (e) Gangjee, A.; Zhao, T.; Lin, L.; Raghavan, S.; Roberts, E. G.; Risinger, A. L.; Hamel, E.; Mooberry, S. L. Synthesis and discovery of water-soluble microtubule targeting agents

that bind to the colchicine site on tubulin and circumvent Pgp mediated resistance. *J. Med. Chem.* **2010**, *53*, 8116–8128. (f) Schobert, R.; Biersack, B.; Dietrich, A.; Effenberger, K.; Knauer, S.; Mueller, T. 4-(3-Halo/amino-4,5-dimethoxyphenyl)-5-aryloxazoles and -*N*-methylimidazoles that are cytotoxic against combretastatin A-4 resistant tumor cells and vascular disrupting in a cisplatin resistant germ cell tumor model. *J. Med. Chem.* **2010**, *53*, 6595–6602. (g) Lee, J.; Kim, S. J.; Choi, H.; Kim, Y. H.; Lim, I. T.; Yang, H.-M.; Lee, C. S.; Kang, H. R.; Ahn, S. K.; Moon, S. K.; Kim, D.-H.; Lee, S.; Choi, N. M.; Lee, K. J. Identification of CKD-516: a potent tubulin polymerization inhibitor with marked antitumor activity against murine and human solid tumors. *J. Med. Chem.* **2010**, *53*, 6337–6354. (h) Romagnoli, R.; Baraldi, P. G.; Cruz-Lopez, O.; Cara, C. L.; Carrion, M. D.; Brancale, A.; Hamel, E.; Chen, L.; Bortolozzi, R.; Basso, G.; Viola, G. Synthesis and antitumor activity of 1,5-disubstituted 1,2,4-triazoles as cis-restricted combretastatin analogues. *J. Med. Chem.* **2010**, *53*, 4248–4258. (i) Jourdan, F.; Leese, M. P.; Dohle, W.; Hamel, E.; Ferrandis, E.; Newman, S. P.; Purohit, A.; Reed, M. J.; Potter, B. V. L. Synthesis, antitubulin, and antiproliferative SAR of analogues of 2-methoxyestradiol-3,17-*O,O*-bis-sulfamate. *J. Med. Chem.* **2010**, *53*, 2942–2951. (j) Lee, L.; Robb, L. M.; Lee, M.; Davis, R.; Mackay, H.; Chavda, S.; Babu, B.; L.; O'Brien, E.; Risinger, A. L.; Mooberry, S. L.; Lee, M. Design, synthesis, and biological evaluations of 2,5-diaryl-2,3-dihydro-1,3,4-oxadiazoline analogs of combretastatin-A4. *J. Med. Chem.* **2010**, *53*, 325–334. (k) Bonezzi, K.; Taraboletti, G.; Borsotti, P.; Bellina, F.; Rossi, R.; Giavazz, R. Vascular disrupting activity of tubulin-binding 1,5-diaryl-1*H*-imidazoles. *J. Med. Chem.* **2009**, *52*, 7906–7910. (l) Wu, Y.-S.; Coumar, M. S.; Chang, J.-Y.; Sun, H.-Y.; Kuo, F.-M.; Kuo, C.-C.; C., Y.-J.; Chang, C.-Y.; Hsiao, C.-L.; Liou, J.-P.; Chen, C.-P.; Yao, H.-T.; Chiang, Y.-K.; Tan, U.-K.; Chen, C.-T.; Chu, C.-Y.; Wu, S.-Y.; Yeh, T.-K.; Lin, C.-Y.; Hsieh, H.-P. Synthesis and evaluation of 3-aroylindoles as anticancer agents: metabolite approach. *J. Med. Chem.* **2009**, *52*, 4941–4945. (m) Ty, N.; Dupeyre, G.; Chabot, G. G.; Seguin, J.; Tillequin, F.; Scherman, D.; Michel, S.; Cahcet, X. *Bioorg. Med. Chem.* **2008**, *16*, 7494–7503. (n) Chiang, Y.-K.; Kuo, C.-C.; Wu, Y.-S.; Chen, C.-T.; Coumar, M. S.; Wu, J.-S.; Hsieh, H.-P.; Chang, C.-Y.; Jseng, H.-Y.; Wu, M.-H.; Leou, J.-S.; Song, J.-S.; Chang, J.-Y.; Lyu, P.-C.; Chao, Y.-S.; Wu, S.-Y. Generation of ligand-based pharmacophore model and virtual screening for identification of novel tubulin inhibitors with potent anticancer activity. *J. Med. Chem.* **2009**, *52*, 4221–4233.

(5) (a) Max, M. A. Small-molecule, tubulin-binding compounds as vascular targeting agents. *Expert Opin. Ther. Pat.* **2002**, *12*, 769–776. (b) Tozer, G. M.; Kanthou, C.; Baguley, B. C. Disrupting tumour blood vessels. *Nat. Rev. Cancer* **2005**, *5*, 423–435. (c) Siemann, D. W.; Chaplin, D. J.; Horsman, M. R. Vascular targeted therapies for treatment of malignant disease. *Cancer* **2004**, *100*, 2491–2499. (d) Kanthou, C.; Tozer, G. M. The tumor vascular targeting agent combretastatin A-4 phosphate induces reorganization of the actin cytoskeleton and early membrane blebbing in human endothelial cells. *Blood* **2002**, *99*, 2060–2069. (e) Young, S. L.; Chaplin, D. J. Combretastatin A4 phosphate: background and current clinical status. *Expert Opin. Invest. Drugs* **2004**, *13*, 1171–1182. (f) Nagaiah, G.; Remick, S. C. Combretastatin A4 phosphate: a novel vascular disrupting agent. *Future Oncol.* **2010**, *6*, 1219–1228. (g) McKeage, M. J.; Baguley, B. C. Disrupting established tumor blood vessels: an emerging therapeutic strategy for cancer. *Cancer* **2010**, *116*, 1859–1871. (h) Kanthou, C.; Tozer, G. M. Tumour targeting by microtubule-depolymerising vascular disrupting agents. *Expert Opin. Ther. Targets* **2007**, *11*, 1443–1457. Schwartz, E. L. Antivascular actions of microtubule-binding drugs. *Clin. Cancer Res.* **2009**, *15*, 2595–2601. (i) Chaplin, D. J.; Dougherty, G. J.; Siemann, D. W. Vascular disrupting agents. *Antiangiogenic Cancer Ther.* **2008**, 329–364. (j) Siemann, D. W.; Chaplin, D. J.; Walicke, P. A. A review and update of the current status of the vasculature-disabling agent combretastatin-A4 phosphate (CA4P). *Expert Opin. Invest. Drugs* **2009**, *18*, 189–197.

(6) *Vascular-Targeted Therapies in Oncology*; Siemann, D. W., Ed.; John Wiley and Sons: New York, 2006.

(7) (a) Patnaik, P. *A Comprehensive Guide to the Hazadous Properties of Chemical Substances*; John Wiley & Sons: Hoboken, NJ, 2007; p 229.

(b) IPCS INCHEM. Colchicine. http://www.inchem.org/documents/pims/pharm/colchic.htm.

(8) Kang, G.-J.; Getahun, Z.; Muzaffar, A.; Brossi, A.; Hamel, E. *N*-Acetylcolchinol *O*-methyl ether and thiocolchicine, potent analogs of colchicine modified in the C ring. *J. Biol. Chem.* **1990**, *256*, 10255–10259.

(9) Niel, E.; Scherrmann, J.-M. Colchicine today. *Jt., Bone, Spine* **2006**, *73*, 672–678.

(10) (a) Blakey, D. C.; Ashton, S. E.; Westwood, F. R.; Walker, M.; Anderson, J. R. ZD6126: a novel small molecule vascular targeting agent. *Int. J. Radiat. Oncol., Biol., Phys.* **2002**, *54*, 1497–1502. (b) Davis, P. D.; Dougherty, G. J.; Blakey, D. C.; Galbraith, S. M.; Tozer, G. M.; Holder, A. L.; Naylor, M. A.; Nolan, J.; Stratford, M. R. L.; Chaplin, D. J.; Hill, S. A. ZD6126: a novel vascular-targeting agent that causes selective destruction of tumor vasculature. *Cancer Res.* **2002**, *62*, 7247–7253.

(11) (a) LoRusso, P. M.; Gadgeel, S. M.; Wozniak, A.; Barge, A. J.; Jones, H. K.; DelProposto, Z. S.; DeLuca, P. A.; Evelhoch, J. L.; Boerner, S. A.; Wheeler, C. Phase I clinical evaluation of ZD6126, a novel vascular-targeting agent, in patients with solid tumors. *Invest. New Drugs* **2008**, *26*, 159–167. (b) Beerepoot, L. V.; Radema, S. A.; Witteveen, E. O.; Thomas, T.; Wheeler, C.; Kempin, S.; Voest, E. E. Phase I clinical evaluation of weekly administration of the novel vascular-targeting agent, ZD6126, in patients with solid tumors. *J. Clin. Oncol.* **2006**, *24*, 1492–1498. (c) Rustin, G. J.; Shreeves, G.; Nathan, P. D.; Gaya, A.; Ganesan, T. S.; Wang, D.; Boxall, J.; Poupard, L.; Chaplin, D. J.; Stratford, M. R. L.; Balkissoon, J.; Zweifel, M. A phase Ib trial of CA4P (combretastatin A-4 phosphate), carboplatin, and paclitaxel in patients with advanced cancer. *Br. J. Cancer* **2010**, *102*, 1355–1360 and references therein.

(12) A number of other VDA agents have also entered clinical trials: (a) Lickliter, J. D.; Francesconi, A. B.; Smith, G.; Burge, M.; Coulthard, A.; Rose, S.; Griffin, M.; Milne, R.; McCarron, J.; Yeadon, T.; Wilks, A.; Cubitt, A.; Wyld, D. K.; Vasey, P. A. Phase I trial of CYT997, a novel cytotoxic and vascular disrupting agent. *Br. J. Cancer* **2010**, *103*, 597–606. (b) Mita, M. M.; Spear, M. A.; Yee, L. K.; Mita, A. C.; Heath, E. I.; Papadopoulos, K. P.; Federico, K. C.; Reich, S. D.; Romero, O.; Malburg, L.; Pilat, M.-J.; Lloyd, G. K.; Neuteboom, S. T. C.; Cropp, G.; Ashton, E.; LoRusso, P. M. Phase 1 first-in-human trial of the vascular disrupting agent plinabulin (NPI-2358) in patients with solid tumors or lymphomas. *Clin. Cancer Res.* **2010**, *16*, 5892–5899. (c) Baguley, B. C.; McKeage, M. J. ASA404: a tumor vascular-disrupting agent with broad potential for cancer therapy. *Future Oncol.* **2010**, *6*, 1537–1543. (d) Hinnen, P.; Eskens, F. A. L. M. Vascular disrupting agents in clinical development. *Br. J. Cancer* **2007**, *96*, 1159–1165. (e) Lippert, J. W. Vascular disrupting agents. *Bioorg. Med. Chem.* **2007**, *15*, 605–615.

(13) Rojiani, M. V.; Rojiani, A. M. Morphologic Manifestations of Vascular-Disrupting Agents in Preclinical Models. In *Vascular-Targeted Therapies in Oncology*; Siemann, D. W., Ed.; John Wiley and Sons: New York, 2006; pp 81−94.

(14) Shi, W.; Horsman, M. R.; Siemann, D. W. Combined Modality Approaches Using Vasculature-Disrupting Agents. In *Vascular-Targeted Therapies in Oncology*; Siemann, D. W., Ed.; John Wiley and Sons: New York, 2006; pp 123−136.

(15) Hua, J.; Sheng, Y.; Pinney, K. G.; Garner, C. M.; Kane, R. R.; Prezioso, J.; Pettit, G. R.; Chaplin, D. J.; Edvardsen, K. Oxi4503, a novel vascular targeting agent: effects on blood flow and antitumor activity in comparison to combretastatin A-4 phosphate. *Anticancer Res.* **2003**, *23*, 1433–1440.

(16) Kremmidiotis, G.; Leske, A. F.; Lavranos, T. C.; Beaumont, D.; Gasic, J.; Hall, A.; O'Callaghan, M.; Matthews, C. A.; Flynn, B. L. BNC105: a novel tubulin polymerization inhibitor that selectively disrupts tumor vasculature and displays single-agent antitumor efficacy. *Mol. Cancer Ther.* **2010**, *9*, 1562–1573.

(17) Aspects of the work presented in this report have been drawn from our published patents: (a) Chaplin, J. H.; Gill, G. S.; Grobelny, D. W.; Flynn, B. L. Preparation of Benzofurans and Related Derivatives as Tubulin Polymerization Inhibitors for Treating Neoplasm and Inflammation. PCT Int. Appl. WO2006084338, 2006. (b) Chaplin, J. H.; Gill, G. S.; Grobelny, D. W.; Flynn, B. L.; Kremmidiotis, G.

Substituted Benzofurans, Benzothiophenes, Benzoselenophenes and Indoles and Their Use as Tubulin Polymerization Inhibitors. PCT Int. Appl. WO2007087684, 2007.

(18) (a) Pinney, K. G.; Bounds, A. D.; Dingeman, K. M.; Mocharla, V. P.; Pettit, G. R.; Bai, R.; Hamel, E. A new anti-tubulin agent containing the benzo[*b*]thiophene ring system. *Bioorg. Med. Chem. Lett.* **1999**, *9*, 1081–1086. (b) Mullica, D. F.; Pinney, K. G.; Mocharla, V. P.; Dingeman, K. M.; Bounds, A. D.; Sappenfield, E. L. Characterization and structural analyses of trimethoxy and triethoxybenzo[*b*]thiophene. *J. Chem. Crystallogr.* **1998**, *28*, 289–295.

(19) Flynn, B. L.; Verdier-Pinard, P.; Hamel, E. A novel palladium-mediated coupling approach to 2,3-disubstituted benzo[*b*]thiophenes and its application to the synthesis of tubulin binding agents. *Org. Lett.* **2001**, *3*, 651–654.

(20) Flynn, B. L.; Flynn, G. P.; Hamel, E.; Jung, M. K. The synthesis and tubulin binding activity of thiophene-based analogues of combretastatin A-4. *Bioorg. Med. Chem. Lett.* **2001**, *11*, 2341–2343.

(21) Flynn, B. L.; Hamel, E.; Jung, M. K. A one-pot synthesis of benzo[*b*]furan and indole inhibitors of tubulin polymerization. *J. Med. Chem.* **2002**, *45*, 2670–2673.

(22) Related indenones I (X = carbonyl) are inactive: Kerr, D. J.; Hamel, E.; Jung, M. K.; Flynn, B. L. The concise synthesis of chalcone, indanone and indenone analogues of combretastatin A4. *Bioorg. Med. Chem.* **2007**, *15*, 3290–3298.

(23) Liou, J.-P.; Chang, Y.-C.; Kuo, F.-M.; Chang, C-.W.; Tseng, H.-Y.; Wang, C.-C.; Yang, Y.-N.; Chang, J.-Y.; Lee, S.-J.; Hsieh, H. P. Concise synthesis and structure—activity relationships of combretastatins A-4 analogues, 1-aroylindoles and 3-aroylindoles, a novel class of potent antitubulin agents. *J. Med. Chem.* **2004**, *47*, 4247–4257.

(24) Chaplin, J. H.; Flynn, B. L. A multi-component coupling approach to benzo[*b*]furans and indoles. *J. Chem. Soc., Chem. Commun.* **2001**, 1594–1595.

(25) Gill, G. S.; Grobelny, D. W.; Chaplin, J. H.; Flynn, B. L. An efficient synthesis and substitution of 3-aroyl-2-bromobenzo[*b*]furans. *J. Org. Chem.* **2008**, *73*, 1131–1134.

(26) Larock, R. C.; Yum, E. K.; Doty, M. J.; Sham, K. C. Synthesis of aromatic heterocycles via palladium-catalyzed annulation of internal alkynes. *J. Org. Chem.* **1995**, *60*, 3270–3271.

(27) Bussolati, B.; Deambrosis, I.; Russo, S.; Deregibus, M. C.; Camussi, G. Altered angiogenesis and survival in human tumor-derived endothelial cells. *FASEB J.* **2003**, *17*, 1159–1161.

(28) Ohsumi, K.; Nakagawa, R.; Fukuda, Y.; Hatanaka, T.; Morinaga, Y.; Nihei, Y.; Ohishi, K.; Suga, Y.; Akiyama, Y.; Tsuji, T. Novel combretastatin analogues effective against murine solid tumors: design and structure—activity relationships. *J. Med. Chem.* **1998**, *41*, 3022–3032.

(29) Maya, A. B. S.; Perez-Melero, C.; Mateo, C.; Alonso, D.; Fernandez, J. L.; Gajate, C.; Mollinedo, F.; Pelaez, R.; Caballero, E.; Medarde, M. Further naphthylcombretastatins. An investigation on the role of the naphthalene moiety. *J. Med. Chem.* **2005**, *48*, 556–568.

(30) Cushman, M.; Nagarathnam, D.; Gopal, D.; Chakraborti, A. K.; Lin, C. M.; Hamel, E. Synthesis and evaluation of stilbene and dihydrostilbene derivatives as potential anticancer agents that inhibit tubulin polymerization. *J. Med. Chem.* **1991**, *34*, 2579–2588.

(31) Subsequent to our published patents on C7-OH benzo-[*b*]furan, benzo[*b*]thiophene, and indole analogues of **11** (ref 17), Cachet and Hseih reported that C7-OH analogues of **15** exhibit reduced potency, albeit to a lesser extent than does a C5-OH analogue (refs 4l and 4m). Additionally, in their earlier report (see ref 23), Hseih and co-workers also observed a modest increase in potency for a C2-methyl analogue of indole **15** (∼2-fold decrease in IC$_{50}$ across multiple cell lines). However, consistent with our findings on benzo[*b*]furans, we have shown that the introduction of *both* C7-OH and C2-Me to **15** affords a much more potent analogue (ref 17b). A more detailed description of the SAR of indoles and other heterocyclic analogues of **8** will be reported elsewhere.

(32) See Supporting Information for a complete listing of benzofurans evaluated.

(33) Ravelli, R. B. G.; Gigant, G.; Curmi, P. A.; Jourdain, I.; Lachkar, S.; Sobel, A.; Knossow, M. Insight into tubulin regulation from a complex with colchicine and a stathmin-like domain. *Nature* **2004**, *428*, 198–202.

(34) Friesner, R. A.; Murphy, R. B.; Repasky, M. P.; Frye, L. L.; Greenwood, J. R.; Halgren, T. A.; Sanschagrin, P. C.; Mainz, D. T. Extra precision glide: docking and scoring incorporating a model of hydrophobic enclosure for protein—ligand complexes. *J. Med. Chem.* **2006**, *49*, 6177–6196.

(35) For other docking studies on tubulin see the following: Soulère, L. Toward docking-based virtual screening for discovering antitubulin agents by targeting taxane and colchicines binding sites. *ChemMedChem* **2009**, *4*, 161–163 and references cited therein.

(36) Goda, K.; Bacso, Z.; Szabo, G. Multidrug resistance through the spectacle of P-glycoprotein. *Curr. Cancer Drug Targets* **2009**, *9*, 281–297.

(37) (a) Battaglia, A.; Bernacki, R. J.; Bertucci, C.; Bombardelli, E.; Cimitan, S.; Ferlini, C.; Fontana, G.; Guerrini, A.; Riva, A. Synthesis and biological evaluation of 2′-methyl taxoids derived from baccatin III and 14β-OH-baccatin III 1,14-carbonate. *J. Med. Chem.* **2003**, *46*, 4822–4825. (b) Martirosyan, A.; Clendening, J. W.; Goard, C. A.; Penn, L. Z. Lovastatin induces apoptosis of ovarian cancer cells and synergizes with doxorubicin: potential therapeutic relevance. *BMC Cancer* **2010**, *10*, 103.

(38) Pettit, G. R.; Rhodes, M. R. Antineoplastic agents 389. New syntheses of the combretastatin A-4 prodrug. *Anti-Cancer Drug Des.* **1998**, *13*, 183–191.

(39) See Supporting Information for pharmacokinetic studies on the in vivo conversion of **9** to **8**.

(40) The maximum tolerated dose (MTD) for **9** and **5** was determined to be 80 and 300 mg/kg, respectively, and is based on a no observable adverse effect level (NOAEL).

(41) Bionomics. BNC105. http://www.bionomics.com.au/page.php?section=103.

(42) (a) Hamel, E.; Lin, C. M. Synthesis and evaluation of stilbene and dihydrostilbene derivatives as potential anticancer agents that inhibit tubulin polymerization. *Biochemistry* **1984**, *23*, 4173–4184. (b) Hamel, E. Evaluation of antimitotic agents by quantitative comparisons of their effects on the polymerization of purified tubulin. *Cell Biochem. Biophys.* **2003**, *38*, 1–22.

(43) Verdier-Pinard, P.; Lai, J.-Y.; Yoo, H.-D.; Yu, J.; Márquez, B.; Nagle, D. G.; Nambu, M.; White, J. D.; Falck, J. R.; Gerwick, W. H.; Day, B. W.; Hamel, E. Structure—activity analysis of the interaction of curacin A, the potent colchicine site antimitotic agent, with tubulin and effects of analogs on the growth of MCF-7 breast cancer cells. *Mol. Pharmacol.* **1998**, *53*, 62–76.